November 2022

Neroimaging of Brain Activaion Using Diffuse Optical Tomography

Jingyu Huang
University of South Florida

Neuroimaging of Brain Activation Using Diffuse Optical Tomography

by

Jingyu Huang

A dissertation submitted in partial fulfillment
of the requirements for the degree of
Doctor of Philosophy
Department of Medical Engineering
College of Engineering
University of South Florida

Major Professor: Huabei Jiang, Ph.D.
Robert Frisina Jr., Ph.D.
Mark Jaroszeski, Ph.D.
Michael Weng, Ph.D.
Alexis Cohen-Oram, Ph.D.

Date of Approval:
November 23, 2022

Keywords: Noninvasive Brain Imaging, Repetitive Transcranial Magnetic Stimulation, Healthy Subjects, Depressed Patient, Delirium Patient

Dedication

This dissertation is dedicated to the memory of my father Daiqing Huang; the software Engineer that continue cultivating my sense of curiosity in my young age. I consider myself as an energetic self-motivated person, and I believe those characters are origin from him. In all, thanks to him.

Acknowledgments

I would like to express my sincere gratitude to my advisor Dr. Huabei Jiang for his wisdom and assistance through the course and research. My sincere gratitude also goes to Weng, Michael, the Department of Industrial and Management Systems, College of Engineering for his guidance and wisdom about how to be successful. I am indebted to all my dissertation committee members for their advice and guidance throughout.

I am appreciative to all my professors, my fellow BME graduate students (Spring 2018 intake), and to all my lab mates for their encouragement and generous help. Especially, I would like to thank Dr. Hao Yang for his gift to provide suggestion and advice on the technical issues whenever and whatever I asked.

My appreciation is also extended to my family and friends, who accepted and tolerated me. Without any resentment and audible complaints, my parents always stand on my side and give me the good example during the years when I was depressed and sick. Chelsea, my love, her kindness, support and motivation during this work always become my energy to walk through the dark time. She is a great listener and spiritual guider when I face really challenge. I am particularly appreciative to my mom, Mrs. Li Chen, for cultivating my personality and education.

Finally, I convey my gratitude to all thank-worthy people who have supported and encouraged me throughout my academic carrier and my life.

Table of Contents

List of Tables

List of Figures

Abstract

This research has two parts. The first part focuses on the use of non-invasive imaging technique, diffuse optical tomography (DOT), to study the brain activation during the stimulation in the clinical room. It further extends the application of DOT by using it to monitor the hemodynamic response during the TMS stimulation in different parameters. Diffuse optical tomography (DOT) is based on NIR light that exploits the relative transparency of biological tissue. The part two and three extends the application in the hospital for delirium patient study and arm muscle dystrophy by adding the sources and detectors to monitor the brain and arm simultaneously.

Diffuse optical tomography provides three-dimensional tissue and functional information with high spatial resolution and excellent contrast. With the application on brain combined with repetitive transcranial magnetic stimulation (rTMS), we detect the different hemodynamic response with different resting motor threshold (rMT) stimulation parameters for healthy subjects. In a functional imaging approach, we study the hemodynamic changes and volumetric location of hemodynamic response. By doing so, we hope to project the tomography imaging as a cost effective and less harmful alternative imaging modality for the brain stimulation imaging. We propose a 100% rMT TMS stimulation for both healthy subjects and depressed patients.

In the first part, by using diffuse optical tomography, we guide its application and monitor the hemodynamic response successfully. With the comparison of hemodynamic response between healthy subjects and depressed patients in different views, it is useful for studying the mechanism of TMS and the pathophysiology of the disorders in which it is applied.

After the application for the brain detection during the TMS stimulation, we developed a novel and portable diffuse optical tomography imaging system for brain imaging in the hospital for delirium study. We scanned the delirium patient before and after treatment. Results from the treatments using our system can find different brain activation before and after treatment for the delirium patient. We found the significant difference of brain activation between before and after treatment of delirium patient. By analyzing the brain hemoglobin response for the delirium patient, our DOT system can help the doctor evaluate how delirious the patients are.

Chapter 1: Diffuse Optical Tomography Imaging Background and Literature

1.1 Introduction

Diffuse optical tomography (DOT) is a noninvasive imaging technique that exploits the relative transparency of biological tissue to NIR light. In DOT, multi-spectral NIR light sequentially excites the tissue at multiple locations and the scattered light is measured at multiple positions along the scalp in the case of brain imaging. The measured multispectral light is then used to reconstruct the spatial distribution of tissue absorption and scattering coefficients at each wavelength through a light propagation model in tissue. The images of absorption and scattering spectra are, respectively, used to derive the images of functional parameters (via the Beer-Lambert law) and cellular morphology (via particle scattering theory). DOT has been used to measure hemodynamic evoked response in several cortical areas both in humans and small animals [1,2]. These studies have proved that DOT is able to image hemodynamic activity with a good spatial resolution comparable to fMRI.

1.1.1 Brief History of Diffuse Optical Tomography Imaging

Diffuse optical tomography (DOT) is an emerging noninvasive imaging modality based on the scattering and absorption properties of non-ionizing near-infrared light in biological tissue. It can be viewed as an extension and improvement to fNIRS, similar to the distinction between magnetic resonance spectroscopy and magnetic resonance imaging [6]. As the NIR light is poorly absorbed relatively by tissue, light can penetrate through the tissue up to several centimeters [3]. Using multiple near-infrared wavelengths, it is able to accurately measure absolute and relative deoxygenated ([Hb]), oxygenated ([HbO]), and total hemoglobin ([HbT]) concentrations. Most

pertinently, it combines multi-channel data acquisition with sophisticated image reconstruction algorithms to produce quantitative three-dimensional images of changes in regional blood volume and oxygenation at high temporal and spatial resolutions [4]. Oxy-hemoglobin and deoxy-hemoglobin are the two major absorbers. Thus, the two wavelengths we used (780nm and 850 nm) are ideally suited for brain imaging to achieve a high signal-to-noise ratio [5]. Over the past 15 years, DOT has been successfully utilized in imaging epilepsy, breast cancer, osteoarthritis, and cortical activation [6]. It has been well documented that DOT is able to image hemodynamic activity with a spatial resolution comparable to fMRI.

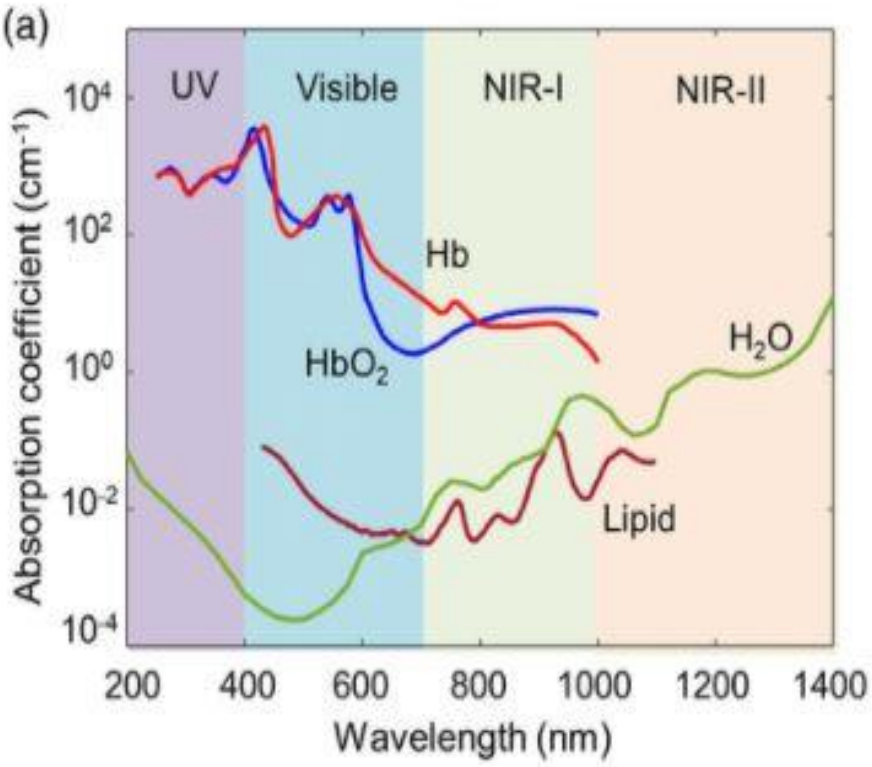

Figure 1.1 Absorption coefficient spectra of various tissue chromophores

1.2 Physics of the Diffuse Optical Tomography Imaging

In diffuse optical tomography (DOT), the photon diffusion/transport model establishes the mathematical relationship between the imaging parameters and the observable/computable photon

density, which providing a tractable basis for image reconstruction [7]. The most used wavelengths in DOT imaging for tissue excitation are the near infrared (NIR) region from 700nm ~ 900nm, which offering penetration depths extending to several centimeters. The model is a partial differential or integral equation requiring the numerical methods to solve. Briefly, the photon diffusion Eq. (1.1) below combined with Robin boundary condition Eq. (1.2) are essential in DOT image reconstruction algorithm.

$$\nabla \cdot D(r)\,\nabla \cdot \Phi(r) - \mu_\alpha(r)\Phi(r) = -S(r) \qquad 1.1$$

$$-D(r)\nabla\Phi_n = \alpha\Phi \qquad 1.2$$

$\Phi(r)$ is the photon density, α is the coefficient related to internal reflection at the boundary, $D(r)$ and $\mu_\alpha(r)$ are the diffusion and absorption coefficients, and $S(r)$ is the source term. And the diffusion coefficient is defined as:

$$D(r) = \frac{1}{(\mu_\alpha(r) + \mu_s'(r))} \qquad 1.3$$

where $\mu_s'(r)$ is the reduced scattering coefficient. The objective of the DOT reconstruction algorithm is to recover $\mu_\alpha(r)$ and $\mu_s'(r)$ at all positions inside the computational domain, achieved through a regularized Newton's method to update an initial optical property distribution iteratively to minimize a weighted sum of the squared difference between computed and measured optical data along its boundary. A calibration method was applied to reduce the errors caused by the use of different source/detection intensities/positions and the system hardware [8]. In this study, we utilize the nonzero photon density and type III boundary condition Eq. (1.2). After making use of finite-element discretization, we can get the matrix representation of Eq (1.1) and get the derived

matrix relationships through differentiation [13]. These equations can lead to an inverse problem solution:

$$[A_{x,m}]\{\Phi_{x,m}\} = \{b_{x,m}\} \quad 1.4$$

$$[A_{x,m}]\left\{\frac{\partial \Phi_{x,m}}{\partial x}\right\} = \left\{\frac{\partial b_{x,m}}{\partial x}\right\} - \left\{\frac{\partial A_{x,m}}{\partial x}\right\}\{\Phi_{x,m}\} \quad 1.5$$

$$\left(\Im_{x,m}^{T}\Im_{x,m} + \lambda I\right)\Delta\chi = \Im_{x,m}^{T}(\Phi_{x,m}^{o} - \Phi_{x,m}^{c}) \quad 1.6$$

where the elements of matrix $[A_{x,m}]$ and the entries in column vectors $\{b_{x,m}\}$ can be expressed by a set of locally spatially varying Lagrangian basis functions; χ expresses $(\Delta D_1, \Delta D_2, \ldots, \Delta D_N, \Delta\mu_{a,1}, \Delta\mu_{a,2}, \ldots, \Delta\mu_{a,N})^T$ is the update vector for the optical property profiles, where N is the total number of nodes in the finite element mesh. $\Im_{x,m}$ is the Jacobian matrix consisting of the derivatives of $\Phi_{x,m}$ with respect to χ at each boundary observation node. *I* is identity matrix; λ may be a scale or a diagonal matrix; $\Phi_{x,m}^{o}$ and $\Phi_{x,m}^{c}$ are the observed and the computed excitation or emission photon density at the boundary sites, respectively [9,10,11]. Optical and fluorescent images are formed by iteratively solving Eqs. (1.4) – (1.6) and updating the optical (D_x and $\mu_{a,x}$) and fluorescent property distributions from presumably uniform initial estimates of these properties. The concentrations of oxy- and deoxy-hemoglobin ([HbO] and [Hb]) were then calculated using the recovered absorption coefficients at both wavelengths based on the Beer-Lambert law [12]. Coupled with a least-square fitting procedure and pseudo inverse matrix calculation, hemoglobin concentration, [HbT], was calculated by summing up [HbO] and [Hb] which is proportional to cerebral blood volume (CBV) [13].

The aim and idea for the algorithm utilized in the DOT image reconstruction would focus on how to generate the parameters and transfer the photon equation to inverse problem. With the solution of the inverse problem, we can have the distribution of absorption coefficient.

1.3 Diffuse Optical Tomography Configuration and Instrumentation

1.3.1 Configuration

We used a fast multispectral DOT system for optical signal recording, as described in detail previously (Figure 1.2A). The computer sent a starting signal to the FPGA to sequentially light up two groups of LEDs (96 LEDs, 48 LEDs for each group,780nm and 850nm). The light signal was delivered to interface through optical fibers. The diffused light signal was received by the detection optical fibers and it was converted to electrical signals and collected by the data acquisition boards (DAQ). The system performs continuous-wave (CW) measurements using 48 light-emitting diodes (LEDs) as the excitation sources and highly sensitive photodetectors as the light detectors. Forty-eight optical source/detector pairs were distributed the brain and attached firmly to the scalp. The blue dots in represent the locations of detectors and the red dots represent the locations of the sources. The average distance between 2 adjacent source-detector positions was nearly 1 cm with 0.32 variance. The sources/detectors were also attached to a two-layer interface coupled with a 256-channel medium size EEG cap which fits all the head sizes of the participants in this study. Tomographic optical data were collected with a temporal resolution of 14.4 Hz at two NIR wavelengths (780 and 850 nm). The raw optical data from all channels were inspected to exclude the epochs with significant discontinuity due to the motion artifacts during the measurement. After excluding the suspected ‘discontinuous channels’, a blackmanharris window-based finite impulse response filter was applied to remove the instrumental noise after the data collection from the DAQ. The data was extracted and filtered in Matlab [13].

1.3.2 LED

Two groups of high-power NIR LEDs at wavelengths of 780nm and 850nm were chosen as the light sources. The rising and falling time of the LED is less than 50 ns [14]. The pulse width is 10 μs. Radiant Power is around 1.6 W to ensure the energy for the light signal. 48 pairs of LEDs with 780nm and 850nm were controlled by the self-designed LED driver to make sure the rising and falling time can be compatible with the data acquisition system. Table 1. shows the parameters for these LEDs.

Table 1.1 Wavelength of LEDs for DOT imaging system

Model number	Wavelength	Half Band Width	Radiant Power	Manufacturer
SMB780	780nm	25nm	1.65 W(I_{FP}=4A)	Marubeni
SMB850D	850nm	20nm	1.60W (I_{FP}=3A)	Marubeni

I_{FP}：Pulse forward current, duty=1%, pulse width=10μs

1.3.3 Detection Units

The detectors were chosen to cover a large dynamic detection range. The high sensitivity avalanche photodiode detectors C5460-1 consists of an APD and a low-noise current-to-voltage amplifier, which is suitable for low-light-level detection. The photon sensitivity at 30dB is 1.5×108 V/W and the electronic noise level is 1 mV. The noise equivalent intensity is 6.7pW. Since the maximum output voltage is about 10V, accordingly the maximum detectable light power is 67nW [9].

1.3.4 Interface

The interface for the human brain data acquisition was made by two layers bell shape 3D printing materials which presented in the Figure 1.2 C. The advanced human head interface was designed and implemented by a two-layer structure coupled with a modified 256-channel medium size EEG cap (Figure.1.2 (C)) to hold the source/detector optic fiber bundles that have direct contact with the head. Figure 1.2 (C) shows human subjects wearing the interface during experiments. Experiments have demonstrated that our 3-layer interface was capable of long-term monitoring on human subjects without signal distortion, motion artifact, and discomfort from the subjects.

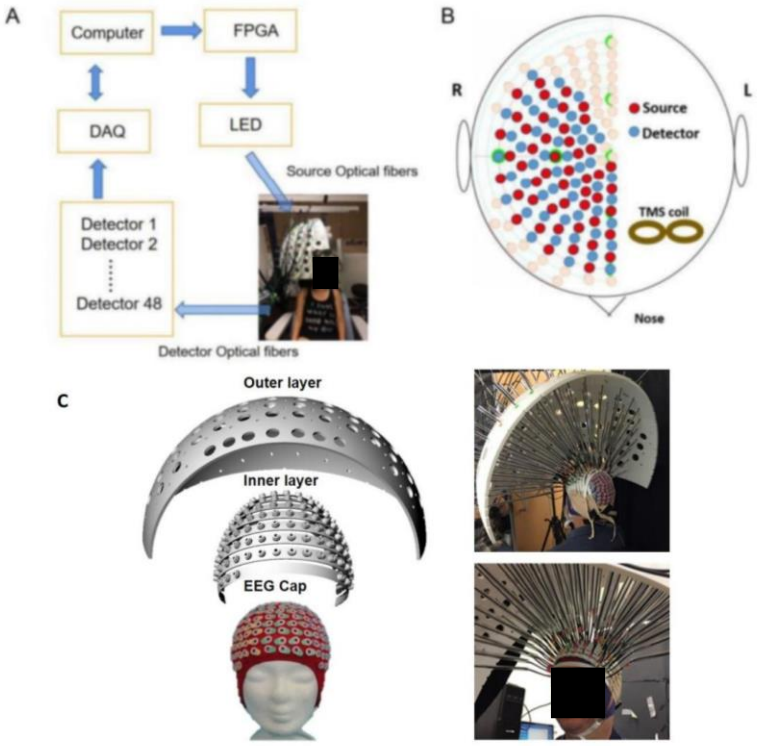

Figure 1.2 Schematic of original DOT imaging system. A) DOT hardware set up. B) Locations of the DOT sources and detectors over the brain surface. A total of 48 source-detector pairs placed on the interest of area. C) Two-layer DOT human brain interface with inner EEG cap.

1.4 Portable Diffuse Optical Tomography Imaging System

Equation 1.2 and 1.3 show that the initial photon distribution depends on the optical energy deposition and scattering, which in turn depends on optical absorption and scatter parameters. Thus, the tomography imaging contrast depends on the optical absorption. This means that, materials which strongly absorb light will produce excellent contrast during the photon transmission. As the Figure 1.1 presented, light absorbers are typically tissue chromophores such as hemoglobin, melanin, lipids, water etc. If we need want to enhance the imaging contrast, we need to concentrate more sources and detectors at the interest of area. With sources and detectors covered, the region of interest would be calculated and get the distribution of brain absorb efficiency.

Portable diffuse optical tomography imaging is based on optical absorption spectroscopy which attempts to identify the absorb efficiency with multiple wavelengths. The selected wavelengths are such that the different absorber can be distinguished from each other. After multiwavelength imaging, the resulting set of DOT images at each single wavelength are sent into a spectral algorithm, where they are converted to the value of hemoglobin concentration [15].

The significant innovative design for the portable system is the development of brain interface. New interface was designed to be suitable for the hospital environment and had to discard the previous inner and outer layer. To make the whole system more portable, the previous complicated brain interface was replaced by a flexible swimming 3D printing rubber made cap. The relative locations for sources and detectors were based on the 256 channels EEG cap. All the coordinates system were strictly following the previous system. Only the interface and optical fiber bundles were changed to be lighter material and design. The gravity of optical fiber bundles was supported by the home-made arm. By the way, the NIR light alignment use the self-designed

adapters to be rotated 90 degrees. In this case, the big interface was changed and the whole hardware were fastened in a moveable cart. With the installation of 4 wheels, the portable DOT imaging system can be adapted to the hospital environment.

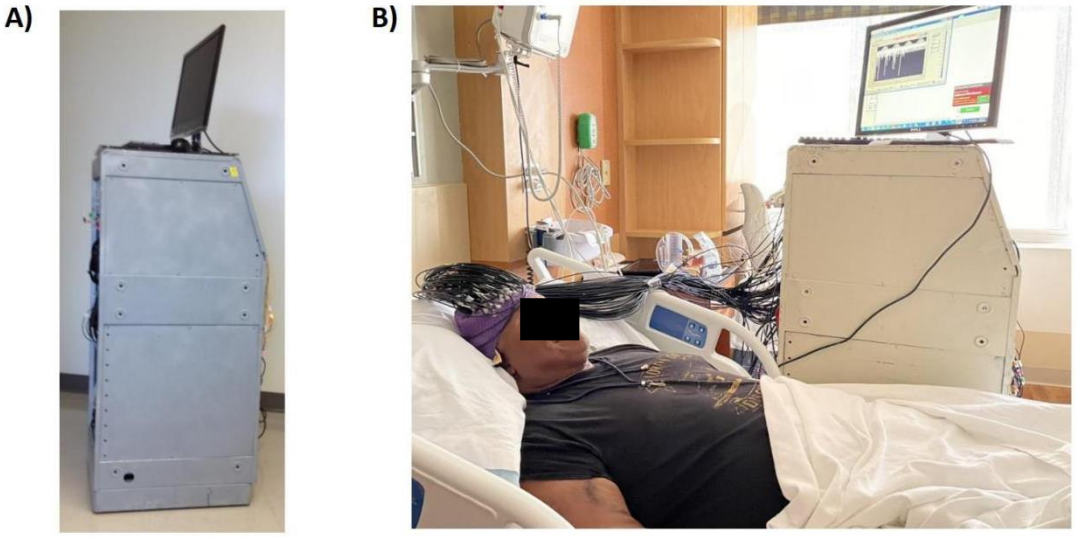

Figure 1.3 Portable DOT imaging system. A) Photo of the portable DOT set up. B) Portable DOT imaging system data acquisition in the hospital environment.

1.5 References

1. Ou W, Nissilä I, Radhakrishnan H, Boas DA, Hämäläinen MS, Franceschini MA. Study of neurovascular coupling in humans via simultaneous magnetoencephalography and diffuse optical imaging acquisition. *Neuroimage*, 2009 Jul 1;46(3):624-32.

2. Brian Mohlenhoff, Melissa Romeo, Max Diem, Bayden R. Wood, Mie-Type. Scattering and Non-Beer-Lambert Absorption Behavior of Human Cells in Infrared Microspectroscopy. *Biophysical Journal*, Volume 88, Issue 5,2005, Pages 3635-3640, ISSN 0006-3495.

3. Scarapicchia Vanessa, Brown Cassandra, Mayo Chantel, Gawryluk Jodie R. Functional Magnetic Resonance Imaging and Functional Near-Infrared Spectroscopy: Insights from Combined Recording Studies. *Frontiers in Human Neuroscience*, Volume,11,2017.

4. Austin T, P. Gibson A, Branco G, Md. Yusof, R. Arridge S, H. Meek J.S., Wyatt D.T, Delpy J, Hebden C. Three-dimensional optical imaging of blood volume and oxygenation in the neonatal brain. *NeuroImage*, Volume 31, Issue 4,2006, Pages 1426-1433, ISSN 1053-8119.

5. Xu Cui, Signe Bray, Allan L. Reiss. Functional near infrared spectroscopy (NIRS) signal improvement based on negative correlation between oxygenated and deoxygenated hemoglobin dynamics. *NeuroImage*, Volume 49, Issue 4, 2010, Pages 3039-3046, ISSN 1053-8119.

6. Jiang S, Huang J, Yang H. *et al.* Neuroimaging of depression with diffuse optical tomography during repetitive transcranial magnetic stimulation. *Sci Rep* 11, 7328 (2021).

7. Ansari MA, Erfanzadeh M, Hosseini Z, Mohajerani E. Diffuse optical tomography: image reconstruction and verification. *J Lasers Med Sci.* 2014 Winter, 5(1):13-8. PMID: 25606334; PMCID: PMC4290522.

8. Rodríguez-Navarro D, Lázaro-Galilea J.L, Bravo-Muñoz I, Gardel-Vicente A, Tsirigotis G. Analysis and Calibration of Sources of Electronic Error in PSD Sensor Response. *Sensors*, 2016; 16(5):619.

9. Yang H, Zhang T, Yang H and Jiang H. Fast multispectral diffuse optical tomography system for in vivo three-dimensional imaging of seizure dynamics. *Appl.Optics,* 2012,51,3461.

10. Dai X, Zhang T, Tang J, R.Carney P and Jiang H. Fast noninvasive functional diffuse optical tomography for brain imaging. *J. Biopotonics,* 2017, e201600267

11. Zhang, J. Zhou, P.R.Carney and H.Jinag. Towards real-time detection of seizures in aware rate wit GPU-Accelerated diffuse optical tomography. *Journal of Neuroscience Methods,* 2015, 240,28-36.

12. Sassaroli Angelo, and Sergio Fantini. Comment on the modified Beer–Lambert law for scattering media. *Phys. Med. Biol, 2007 Volume* 49, N255.

13. Huang, Jingyu et al. Three-dimensional Optical Imaging of Brain Activation During Transcranial Magnetic Stimulation. *Journal of X-ray science and technology*, 1 Jan. 2021: 891 – 902.

14. Jianjun Yang, Tao Zhang, Hao Yang, and Huabei Jiang. Fast multispectral diffuse optical tomography system for in vivo three-dimensional imaging of seizure dynamics. *Appl. Opt.* 51, 3461-3469 (2012).

15. Hao Yang Wu, Andrew Filer, Iain Styles, and Hamid Dehghani. Development of a multi-wavelength diffuse optical tomography system for early diagnosis of rheumatoid arthritis: simulation, phantoms and healthy human studies. *Biomed. Opt. Express* 7, 4769-4786 (2016).

Chapter 2: TMS, Major Depression and Delirium Background and Literature

2.1. Introduction

2.1.1 Background of Transcranial Magnetic Stimulation

Repetitive transcranial magnetic stimulation (rTMS) is a non-pharmacological, non-invasive brain stimulation technique which is used for various psychiatric disorders. It is also called as TMS for short. When TMS is administered repeatedly at a specific frequency, it is referred to as rTMS. Repetitive TMS (rTMS) has been approved by the FDA since 2008 and it has been proved to be an effective and safe treatment for depression. It involves passing an electrical current through an insulated coil, which creates an alternating magnetic field that penetrates the scalp and skull to induce neuronal depolarization and modulation [1].

Application of high frequency (10-20 Hertz) stimulation of left dorsolateral prefrontal cortex (DLPFC) has an antidepressant effect that can be enhanced by increasing field intensity, increasing the number of stimuli per session, or increasing the number of treatments [2]. However, despite its increasing use, the typical effect sizes have been modest at best.

Though studied the most for major depressive disorder, its use in schizophrenia, posttraumatic stress disorder, substance use disorders, and obsessive-compulsive disorder is also being investigated. Despite ongoing research, our knowledge of the underlying mechanism of rTMS is poorly understood. While rTMS is effective for psychiatric disorders treatment, different antidepressant effect has been reported through the stimulation of left dorsolateral prefrontal cortex (DLPFC) by different field intensity, number of stimuli per session and the number of treatments, and the activation mechanism is largely unclear [3]. Several studies have demonstrated that

approximately 35-40% of patients who do not respond to medications, do respond to subsequent TMS treatment [4]. Despite its observed efficacy, little is known about its mechanism of action. The effectiveness of TMS is likely reduced due to: (1) non-optimized targeting, (2) unclear ideal stimulation parameters (e.g., patterns, frequencies, dosage), and (3) a lack of understanding of how the brain is physiologically responding, during and after, stimulation. As such, neuroimaging with rTMS has been a particularly promising area of research that has been pursued in order to answer these questions [12].

2.1.2 Major Depression

Major depressive disorder is a chronic, recurrent, and debilitating mental health illness linked to significant functional impairment, disability, and mortality [1]. It is the primary and the most common mental disorders in the United States, which is the cause of mental health-related disease burden globally, affecting approximately 300 million individuals [12]. In 2017, an estimated 17.3 million adults had at least one major depressive episode, representing 7.1% of all adults [6,7]. It significantly diminishes psychosocial functioning and overall quality of life. Depression, especially in midlife or beyond, can co-occur with other serious medical illnesses, such as diabetes, cancer, lung disease, heart disease, and Parkinson's disease. These conditions are often worse when depression is present [8]. In 2008, the WHO ranked major depression as the third cause of burden of disease worldwide and projected that this illness will rank first by 2030 [9]. Current research suggests that depression is caused by a combination of genetic, biological, environmental, and psychological factors. Although there have been numerous clinical trials and studies on existing pharmacological and non-pharmacological options, its overall treatment is still challenging [12]. Despite the fact that our knowledge of its underlying pathophysiology has grown

tremendously over the decades, the overall response rates to standard pharmacological treatment options remain underwhelming.

2.2 The Treatment of Depression

The largest and most extensive trial, the Sequenced Treatment Alternatives to Relieve Depression (STAR*D), revealed that antidepressants, even with augmentation, demonstrated suboptimal remission rates. In the treatment of the depression, the remission rates after first treatment with a serotonin re-uptake inhibitor was only 37% [10]. Augmentation with other pharmacological agents such as atypical antipsychotics, lithium, and triiodothyronine has shown to have mixed results, yet are accompanied by significant adverse effects [11]. In lieu of medications then, a concerted effort has been dedicated to studying other treatment options, such as brain stimulation techniques. Transcranial magnetic stimulation (TMS) has now been established over the past decades as a safe and effective treatment for depression [12].

2.3 Brain Imaging During TMS Stimulation

Brain imaging is theoretically able to offer valuable information regarding the above unanswered questions about improving TMS [13]. However, due to the immediate brain changes that occur, only a few modalities possess the temporal resolution required to appropriately evaluate such conditions. Prior studies on brain activation and connectivity during TMS include the usage of functional magnetic resonance imaging (fMRI), magnetoencephalography (MEG), electroencephalography (EEG), and functional near-infrared spectroscopy (fNIRS) [14]. As fMRI, MEG, and EEG use signals that involve the electromagnetic spectrum, their overall resolution and quality are subject to significant measurement artifacts given the fact that TMS produces very strong magnetic and electrical fields. Due to this, fNIRS has been investigated for concurrent imaging as it measures an optical signal, which has no electromagnetic interference [15]. It also

has benefits of being portable, safe, cost-effective, and less restrictive than other devices. However, fNIRS has several technical limitations including scalp interference, shallow imaging depth, low spatial resolution, and an inability to produce three-dimensional images. In this case, the technology with good depth information would be a good choice. Our proposed solution to these problems involves a more novel neuroimaging technique called diffuse optical tomography [12].

2.4 Delirium

2.4.1 Background of Delirium

Delirium is a syndrome of acute brain failure that represents an acute change in awareness, cognition, and attention. The terminology original deviated from the Latin word *delirare*, that represents "to go out of the furrow" [16]. It is a serious neuropsychiatric syndrome that would lead to deficits in attention and cognitive behavior. Although the prevalent and potential life-threating of delirium threaten the quality of the delirium patients' life, the knowledge about the pathogenesis of emergency delirium is limited. The cognitive impairments and damage are highly variant. Memory failure, orientation losing, functional incapacitation, visuospatial ability, and perception are the common phenomenon and symptom that occur in the clinical treatment. Even the social estimated health care cost of delirium in the United States is more than $150 billion every year, the incidence of delirium ranges still existed in a high range.

Delirium can be triggered by a lot of potential reasons and causes. Acute medical illness, drug abuse or withdrawal, and surgery are commonly happening in the clinical. These causes usually deviated from outside of the brain. Certain primary neurological causes like stroke can be recognized as the inside brain problem. In the clinical study, delirium have certain connections with the considerable distress for patients and caregivers [17]. Different people have different delirium duration. Most of the delirium duration would exist a few days, however, the sequelae

symptom specially for episodes persisting would exist for weeks or months in up to 20% of individuals [18,19]. The light symptom for delirium would be treated as the subsyndromal delirium, that describes some patients have delirium features but do not have the criteria for the delirium diagnosis [20,21].

2.4.2 Treatment and Estimation of Delirium

The estimation of delirium based on a high index of suspicion, and it often goes undetected or misdiagnosed [22]. In a study, only 31% of cases were discovered by nursing staff and only 40% of hospital patients referred to a psychiatric consultation [23,24]. Multiple challenges would face when the doctor try to establish the diagnosis of delirium based on the symptoms, cognitive testing, and cognitive functioning. No biomarker with high sensitivity and specificity was considered as the gold standard for the diagnosis of delirium. Although, multiple validated delirium screening tools with high sensitivity and specificity have been used, the mechanism inside is still unknown [25,26].

The treatment goal for delirium should find the cases or triggers. Infection, drug abuse or withdrawal, and surgery are commonly causes for delirium. The treatment of delirium mainly focuses on creating the setting and healing of the body. After calming the brain, the symptom and side effects of delirium could be controlled. The current therapy for delirium has not developed from an understanding of complex neurochemical methods [27]. The choice of the medication often results in the balance between uncertain therapy benefits and adverse effects [28,29]. In all, the use of medication tends to be focused on the treatment of patients with the risk of injury to themselves or others [30,31].

2.5 References

1. Koob, George F., and Michel Le Moal. Drug abuse: hedonic homeostatic dysregulation. *Science*,278, no. 5335 (1997): 52-58.

2. Brigitte Zrenner, Christoph Zrenner, Pedro Caldana Gordon, Paolo Belardinelli, Eric J. McDermott, Surjo R. Soekadar, Andreas J. Fallgatter, Ulf Ziemann, Florian Müller-Dahlhaus. Brain oscillation-synchronized stimulation of the left dorsolateral prefrontal cortex in depression using real-time EEG-triggered TMS. *Brain Stimulation*, Volume 13, Issue 1, 2020, Pages 197-205, ISSN 1935-861X.

3. Bovy, L., Möbius, M., Dresler, M. Combining attentional bias modification with dorsolateral prefrontal rTMS does not attenuate maladaptive attentional processing. *Sci Re* volume 9, 1168 (2019)

4. Higgins ES, George MS. Brain Stimulation Therapies for Clinicians, 2nd ed. Washington, DC, *American Psychiatric Association Publishing*. 2020.

5. George MS, Wassermann EM, Williams WA, Callahan A, Ketter TA, Basser P, Hallett M, Post RM. Daily repetitive transcranial magnetic stimulation (rTMS) improves mood in depression. *Neuroreport.* 1995 Oct 2;6(14):1853-6.

6. Patel V, Chisholm D, Parikh R, Charlson FJ, Degenhardt L, Dua T, Ferrari AJ, Hyman S, Laxminarayan R, Levin C, Lund C, Medina Mora ME, Petersen I, Scott J, Shidhaye R, Vijayakumar L, Thornicroft G, Whiteford H. Addressing the burden of mental, neurological, and substance use disorders: key messages from Disease Control Priorities, 3rd edition. *Lancet*. 2016 Apr 16;387(10028):1672-85.

7. G, Wagner G, Matyas N, Titscher V, Greimel J, Lux L, Gaynes BN, Viswanathan M, Patel S, Lohr KN. Pharmacological and non-pharmacological treatments for major depressive disorder: review of systematic reviews. *BMJ Open.* 2017 Jun 14;7(6): e014912.

8. Https://www.lifeextension.com/protocols/emotional-health/depression

9. Malhi GS, Mann JJ. Depression. *Lancet*. 2018 Nov 24;392(10161):2299-2312. doi: 10.1016/S0140-6736(18)31948-2.

10. Sinyor M, Schaffer A, Levitt A. The sequenced treatment alternatives to relieve depression (STAR*D) trial: a review. *Can J Psychiatry*. 2010 Mar;55(3):126-35.

11. Noah S Philip, Linda L Carpenter, Audrey R Tyrka & Lawrence H Price. Pharmacologic approaches to treatment resistant depression: a re-examination for the modern era. *Expert Opinion on Pharmacotherapy*,11:5, 709-722.

12. Jiang, S., Huang, J., Yang, H. *et al.* Neuroimaging of depression with diffuse optical tomography during repetitive transcranial magnetic stimulation. *Sci Rep* volume 11, 7328 (2021).

13. George MS. Whither TMS: A One-Trick Pony or the Beginning of a Neuroscientific Revolution. *Am J Psychiatry*. 2019 Nov 1;176(11):904-910.

14. Bestmann S, Baudewig J, Siebner HR, Rothwell JC, Frahm J. BOLD MRI responses to repetitive TMS over human dorsal premotor cortex. *Neuroimage*. 2005 Oct 15;28(1):22-9.

15. Kozel FA, Tian F, Dhamne S, Croarkin PE, McClintock SM, Elliott A, Mapes KS, Husain MM, Liu H. Using simultaneous repetitive Transcranial Magnetic Stimulation/functional Near Infrared Spectroscopy (rTMS/fNIRS) to measure brain activation and connectivity. *Neuroimage*. 2009 Oct 1;47(4):1177-84.

16. Wilson JE, Mart MF, Cunningham C, Shehabi Y, Girard TD, MacLullich AMJ, Slooter AJC, Ely EW. Delirium. *Nat Rev Dis Primers*. 2020 Nov 12;6(1):90.

17. Williams ST, Dhesi JK & Partridge JSL, Distress in delirium: causes, assessment and management. *Eur Geriatr Med*,11, 63–70, doi: 10.1007/s41999-019-00276-z (2020).

18. Pandharipande PP et al. Long-term cognitive impairment after critical illness. *The New England journal of medicine*. 2013 Nov, 1306–1316, doi: 10.1056/NEJMoa1301372 (2013).

19. Cole MG et al. Partial and No Recovery from Delirium in Older Hospitalized Adults: Frequency and Baseline Risk Factors. *Journal of the American Geriatrics Society* 63, 2340–2348.

20. Slooter AJC et al. Updated nomenclature of delirium and acute encephalopathy: statement of ten Societies. *Intensive care medicine* 46, 1020–1022.

21. Ouimet S. et al. Subsyndromal delirium in the ICU: evidence for a disease spectrum. *Intensive care medicine* 33, 1007–1013.

22. Thom RP, Levy-Carrick NC, Bui M, Silbersweig D. Delirium. *Am J Psychiatry*. 2019 Oct 1;176(10):785-793.

23. Pisani MA, McNicoll L, Inouye SK. Cognitive impairment in the intensive care unit. *Clin Chest Med,* 2003 Nov; 24:727–737.

24. Farrell KR, Ganzini L. Misdiagnosing delirium as depression in medically ill elderly patients. *Arch Intern Med,* 1995 Feb; 155:2459– 2464.

25. Inouye SK, van Dyck CH, Alessi CA, et al. Clarifying confusion: the Confusion Assessment Method: a new method for detection of delirium. *Ann Intern Med,* 1990; 113:941–948.

26. Bellelli G, Morandi A, Davis DHJ, et al. Validation of the 4AT, a new instrument for rapid delirium screening: a study in 234 hospitalised older people. *Age Ageing* 2014; 43:496–502.

27. Richard S. Bourne, Tayyeb A. Tahir, Mark Borthwick, Elizabeth L. Sampson, Drug treatment of delirium: Past, present and future. *Journal of Psychosomatic Research*, Volume 65, Issue 3, 2008, Pages 273-282.

28. Someya T, Endo T, Hara T, Yagi G, Suzuki J. A survey on the drug therapy for delirium Psychiatry Clin. *Neurosci*, 55 (2001), pp. 397-401.

29. Carnes M, Howell T, Rosenberg M, Francis J, Hildebrand C, Knuppel J. Physicians vary in approaches to the clinical management of delirium. *J Am Geriatr Soc*, 51 (2003), pp. 234-239.

30. Michaud L, Bula C, Berney A, Camus V, Voellinger R, Stiefel F, Burnand B Delirium: guidelines for general hospitals. *J Psychosom Res*, 62 (2007), pp. 371-383.

31. Young J, Inouye SK, *Delirium in older people Br Med J*, 334 (2007), pp. 842-846.

Chapter 3: Portable Diffused Optical Tomography System Design and Validation

3.1 Limitation of Previous DOT System

Considering the recruiting environment, doing experiment in the hospital should have a moveable cart. The previous two-layer large interface needs a huge frame to hang up which is impossible to move in front of patient's room. Guided by the hospital experiment request, we should design a moveable cart and develop the huge interface. As the new device needs to inherit the good resolution and image reconstruction quality, the hardware configuration for the new portable device would still have 48 pairs of sources and detectors which can cover the interest of area. The optical fibers should be manufactured much lighter compared to the previous optical fiber bundles that were made by silica.

Compared to fNRIS, although DOT suffers much less from scalp interface, the presence of hair itself or dark shades impairs the signal quality. As such, pinning or separation of hair is a non-ideal and imprecise method we often employed. As for the hair problem, our optical fibers need to have an extension tip in the end that can insert into the haircut and reach the scalp as near as possible. In this case, the signal would be delivered or received as much as possible instead of absorbing by the haircut.

3.2 New DOT System Design

3.2.1 Optical Fiber Bundle Update

As the system would be applied in the hospital circumstance. Whether the device is moveable becomes the essential aim to guide us how to design and build up the new system. The previous system in the TMS clinical study utilized a large interface because of the heavy mass of

silica optical fiber bundles. In order to achieve the same resolution as the previous device, we still need have 48 sources and 48 detectors made by the plastic optical fiber bundles. The new ordered plastic optical fiber attenuation is 12% less than the previous silica optical fiber and the mass is 45% less than the silica optical fiber. With the new fiber bundles, we discard the large interface and used 3D printer to print out an interface similar to swimming cap size. For guaranteeing the quality of image, the arrangement of sources and detectors were based on the previous pattern.

3.2.2 Interface and Image Setup

In this project, developing a flexible and appropriate brain interface working in the hospital plays an important role in the experiment. our aim focused on the smaller brain interface pattern with good attachment with the scalp. As the figure 3.3 C) shown, a 2-layer structure coupled with a 256-channel medium size EEG was utilized to hold the sources and detectors which have contact directly with the brain surface. The details were introduced previously, and the interface can fit all the head size, which can fasten on the head by a Velcro chin strap [1]. We followed the idea that brain activation can be detected accurately by using an atlas-guided approach without a subject-specific MRI. The 3D finite element mesh for each brain was produced using the brain contour measured a 3D magnetic space digitizer coupled with a head atlas approach. A partial head was selected and transformed into mesh from the whole head atlas which contain the region of interest in the brain (Figure 3.1A). Each subject's locations of 13 landmarks (NZ, IZ, LPA, RPA, CZ, PZ, OZ, T8, C4, Fpz, Fz, T7 and C3) and 48 pairs of source and detector were measured by 3D magnetic space digitizer (Figure 3.1B). Atlas and landmarks of human subject generate subject-specific mesh by affine transformation. In the end, the position of sources and detectors locations were projected to the new subject-specific mesh and it would be used for 3D DOT image reconstruction (Figure 3.1C) [2].

After getting the location of the sources and detectors, the registered mesh would be used in the FET algorithm. This algorithm can calculate the distribution of the absorption coefficient. Each node in the registered mesh can be obtained the value of absorption coefficient. Due to the multiple spectra of the NIR lights, we can use Beer-Lambert law to calculate the relative hemoglobin response for the interest of area.

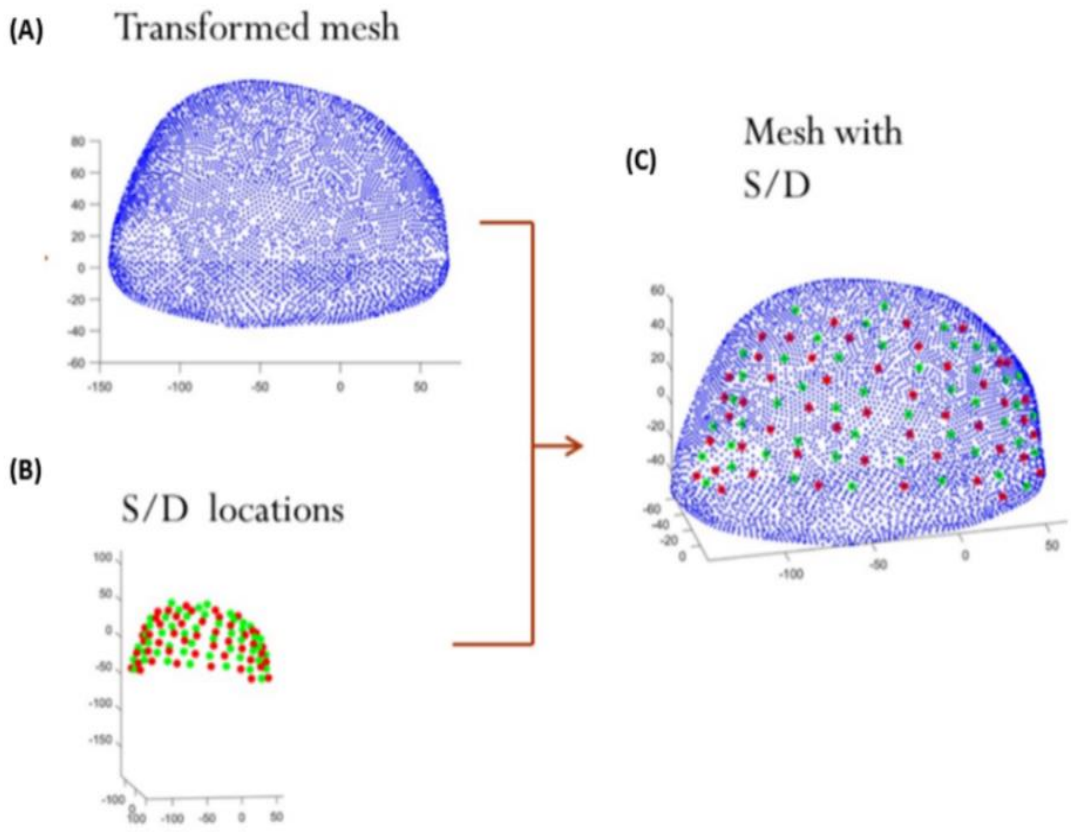

Figure 3.1 Partial transformed mesh with registered sources and detectors. A) Partial transformed mesh from the head Atlas. B) 3D location of 48 pairs of source and detector. C) Projection of 48 pairs of source and detector on the transformed mesh.

3.2.3 Adapter Design

In the TMS study, due to the optical fiber bundles replaced vertically on the scalp, the TMS coil cannot put on the optical fiber bundles that limited our interest of area only in the right prefrontal cortex. When we study the depression mechanism, it is very important to analyze both ipsilateral and contralateral of the brain under TMS stimulation. Thus, the optical bundles need to be replaced horizontally to the brain surface and let the TMS coil above the brain and optical bundles. In this case, we need to design an adapter to guide the optical path and distort the path into 90 degrees. As the figure 3.2 A) shown, we designed an adapter with prism and grin lens to reflect the optical path into 90 degrees. These adapters would be placed and fixed on the 3D printed new interface as the figure 3.2 C shown. The new designed interface would be validated in the brain phantom experiment before the usage in the human study.

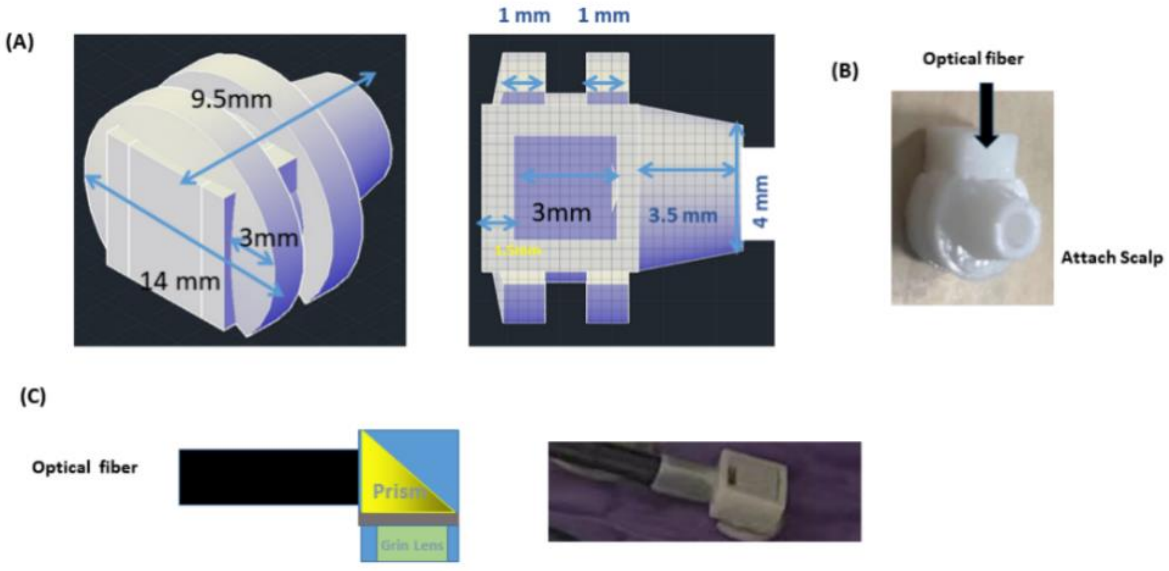

Figure 3.2 Adapter design and interface fiber. A) Sketch of adapter designed by AutoCAD. B) Sample of adapter printed by 3D printing. C) Sketch of prism and grin lens position and photo of adapter connected with interface and fiber.

3.3 Phantom Experiment

Before applying the new DOT system to human study, we performed a tissue-mimicking phantom experiment following the actual steps that we would be taken in human experiments. First of all, a head-shaped phantom was made using an adult head model. The tissue-mimicking phantom was made of TiO2 as the scatterer, the India ink as absorber, and 2% agar as solidification material. With two cylindrical targets (radius = 5mm and height = 5 mm) were placed in the homogeneous background with 0.016 mm-1 absorption coefficient and 1.2mm-1 scattering coefficient. In order to demonstrate the depth-resolving capability of our system, two targets with 2 times higher absorption and scattering coefficients to the background were placed at the depth of 25mm and 35mm below the surface. The new head interface with adapter-connected fiber bundles was placed on the phantom. Followed the same steps of doing human experiment, we got the position information of sources and detectors and recorded optical signals for 780nm and 850nm. In the figure 3.3 B), it shows the reconstructed absorption image at 780nm and the X,Y cut planes are shown in figure 3.3 D) for the 2 targets. In figure 3.3 D), we can clearly detect the targets are located which indicates the depth-solving ability of our new DOT system. With similar image quality obtained at 850nm, we can claim that our DOT system can localize the targets with different optical properties at a depth of at least 35mm.

The brain phantom experiment tries to evaluate the basic imaging function of the new DOT imaging system. With the interest of area located in the prefrontal cortex, our brain phantom was replaced in the prefrontal cortex region. With two located targets in the brain phantom, we can clearly evaluate and find the pros and cons for this device utilized in the neuropsychiatric disorder which is derived from prefrontal cortex.

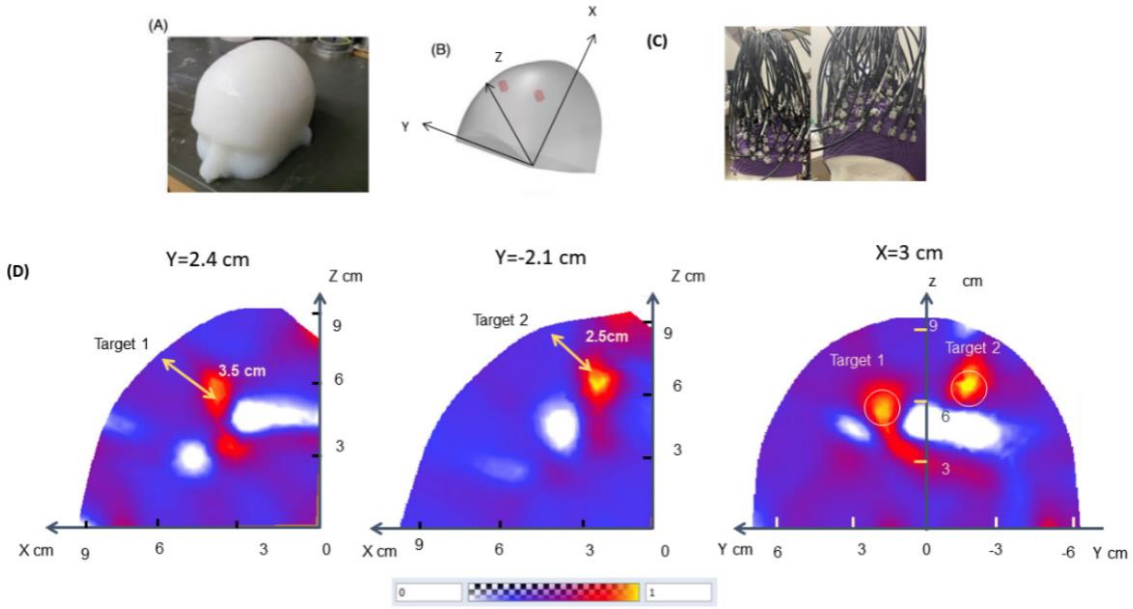

Figure 3.3 Brain phantom experiment. A) Tissue-mimicking head shape phantom. B) Actual target positions. C) Phantom and head interface/fiber bundles. D) Reconstructed absorption image at 780nm for different cut planes.

3.4 Portable DOT Imaging System Human Validation Experiment

3.4.1 Finger Tapping Experiment

The Finger tapping test is widely used to evaluate muscle control and motor ability in the upper extremities around almost a century [3]. This test can be used to quantitatively evaluate Parkinson's disease and some muscle dystrophy disease. Due to its simplicity of construct and execution finger tapping paradigms have long been used in neuroimaging studies for probing motor substrates [4]. In contrast to a large number of publications on finger tapping in adults, few diffuse optical tomography (DOT) studies have examined the functional anatomy of finger tapping in healthy subjects [5]. In this study we presented the reconstructed three-dimensional image to show the hemodynamic of motor cortex during the finger tapping experiment. The primary aims

for this study were moving the DOT toward application in human clinical study, and establish a platform conducting continuous noninvasive DOT function brain mapping for human.

3.4.2 Study Design and Method

All subjects were typical, healthy individuals with no history of neurological disease or learning disability. All subjects were right-handed, and the finger tapping was conducted on the right hand of 3 male university students ranging in age from 20 to 28 years (Mean± SD = 23.45 ± 1.34). The subjects were instructed to tap his index and middle fingers against the thumb at a frequency of 3 Hz without moving the wrist and arm. Each trial contains 30 seconds of stimulation interleaved with 30 seconds of rest. A 1-minute baseline was recorded before each finger-tapping experiment. Each subject was asked to repeat the task using right hand and the recording for each participant lasted 5 minutes in total. No participants data were excluded in this study.

3.4.3 Image Analysis and Processing

The optical absorption coefficients at 780nm and 850nm were used to obtain [HbO] and [Hb] using the Beer-Lambert Law coupled with a least-square fitting procedure followed by pseudo inverse matrix calculation. The concentration of HbT was calculated by summing up [HbO] and [Hb]. [HbT] has been suggested to map cerebral activity in fNIRS for its better spatial specificity than [HbO] or [Hb]. In this study, each trial consisted of 30 seconds of stimulation followed by 30 seconds of rest. In total, the participant was asked to perform 10 trials. An average of 10 trials was used as the final hemodynamic change for each subject. Data analysis was conducted using MATLAB (version R 2017) and SAS (9.4). Subject means were allowed to vary around an individualized intercept across trials with stimulation type as a within subject factor. Redundant analysis was conducted using repeated measures analysis of variance (ANOVA) to allow simpler interpretation of the results. The alpha level was set at 0.05 for all calculations [1].

3.5 Results and Discussion

Hemodynamic activities were observed in the motor cortex when the healthy subjects were performing the right finger-tapping tasks. Figure 3.4 shows the hemodynamic response of healthy subject no.1 indicating the changes of [HbO], [Hb], and [HbT] during the total 10 trials of finger-tapping task. The green, red, and blue lines represent the average of the [HbT], [HbO], and [Hb] for the 10 trials. Each trial of finger tapping generated a precisely time-locked hemodynamic change in the left anatomical motor cortex. Each trial consisted of 30 seconds of resting state followed by 30 seconds finger tapping. After the onset of finger tapping at the 30-second, increased of [HbT] and [HbO] were captured few seconds later. [HbT] and [HbO] reached the peak around the 41^{th} to 42^{th} second. [HbT] decreased sharply to the minimum level within 4 to 7 seconds after the peak, and returned to the baseline in the next 10 seconds. [Hb] started to decrease gradually after the onset of finger tapping 30-second mark and sharply decreased at the around 40^{th} second. After reaching the nadir around 41-second point, [Hb] returned to the baseline in the next 11 seconds.

The finger tapping experiment results focused on monitoring the hemodynamic response for the motor cortex. Due to the motor cortex is the essential part of the brain that participants in the movement, it directly conducts the muscle contraction and finger movement. With 10 trials of the experiment, we can exclude the accidental error. In this case, we can confirm the finger tapping results can prove the ability of our new portable DOT imaging system. By the way, the hemoglobin response results also can be used to compare the image reconstruction results and finish the cross validation.

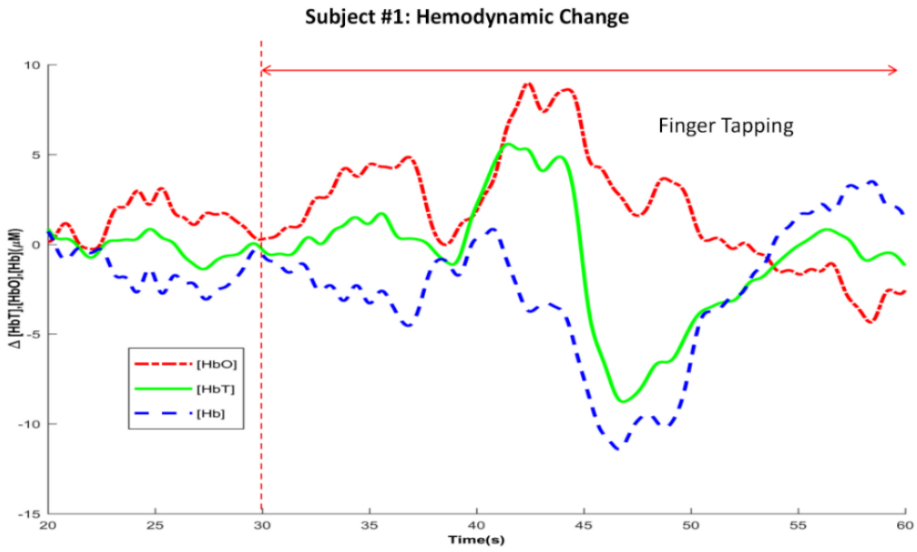

Figure 3.4 Hemodynamic response for finger tapping experiment. Time-locked hemodynamic changes during right-index finger tapping for subject no.1.

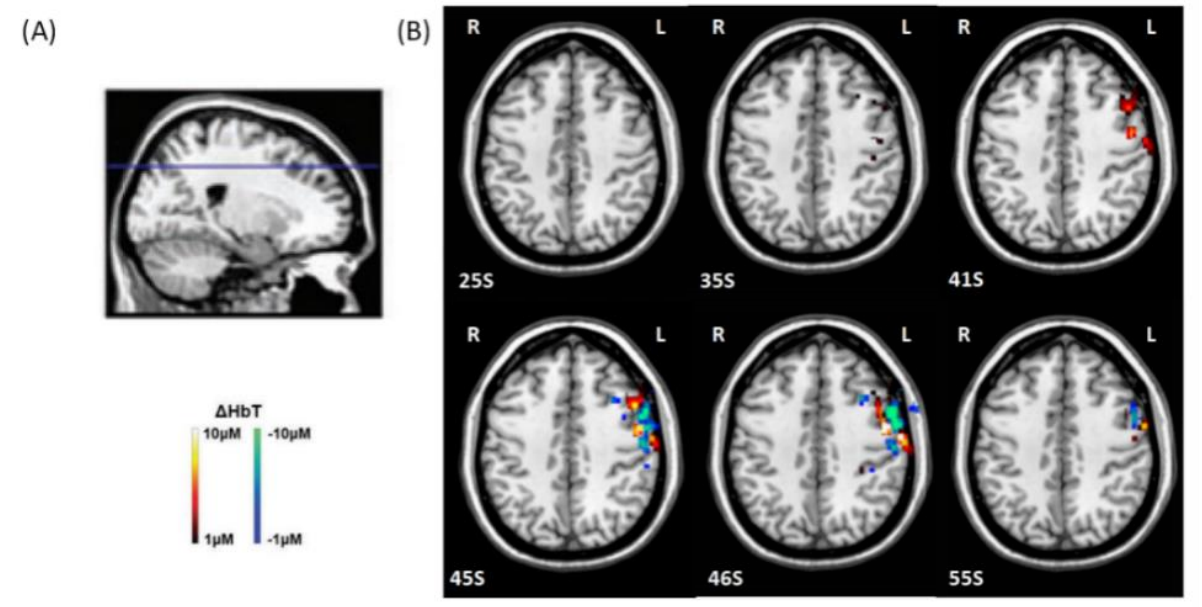

Figure 3.5 Image reconstruction for finger tapping experiment. A) Slice plane indication and color scale bar for the activation maps of subject no.1. B) Transverse section HbT images at selected time pointed for the finger tapping experiment.

Reconstructed [HbT] image was superimposed on the brain MRI of this subject using an open source cross-platform image viewer MRIcron, along with the slice position of brain MRI an the color scale bar of [HbT]. The warm color indicates the increase in [HbT] while the cool color suggests [HbT] decrease. Affine transform was used to register the reconstructed [HbT] space domain to the MRI domain in the MRIcron. The results suggest the activation of left motor cortex during the right-index finger tapping. The results of time-locked hemodynamic changes with time are consistent with previous studies with fMRI, PET and optical imaging, and the brain activities were found at similar cortex locations when motor tasks were performed.

This study confirmed that our new DOT system has ability to map the motor cortex noninvasively in real time. It also helps me understand how to do the DOT lab human study. It validates that DOT is safe for brain imaging without heating the skull, brain or soft tissue and open a gate to do the clinical and hospital human study in the next step.

3.6 DOT and Delirium Study

In the clinical study, the symptom of delirium would occur the brain failure and change the baseline cognitive functioning. Despite how serious and prevalent life-threatening is, the traditional method for detecting the underlying specific mechanisms for delirium is still unknow and limited. With the development of the brain imaging technology, the advancement of neuroimaging in neuropsychiatric disorders offers the possibility of probing the mechanisms and networks involved in delirium. Imaging can be used to quantify normal or pathologic physiology, localize abnormalities to specific brain regions, and offer objective information for diagnostic, preventative, and treatment purposes [6]. Functional techniques in particular may be able to elucidate our understanding of cerebral hemodynamic activity during and after delirium. Previous neuroimaging studies in delirium have utilized modalities such as near-infrared spectroscopy,

functional magnetic resonance imaging, single photon emission computed tomography, positron emission tomography, and transcranial doppler [7]. One of the most pertinent findings reported thus far is significant network dysfunction of the dorsolateral prefrontal cortex and posterior cingulate cortex [8]. Overall though, significant limitations of these techniques and their studies exist and include poor spatial resolution, cost and feasibility, portability, hypoactive subtypes only, and a lack of task-based protocols.

Diffuse optical tomography (DOT) is an emerging noninvasive optical imaging modality that uses near-infrared light to accurately assess changes in brain connectivity. It overcomes the previous limitations due to its inherent algorithms and design and can provide real-time, three-dimensional quantitative imaging data [11,12]. We propose to use DOT to capture images of resting state and task-based neural activity in the bilateral prefrontal cortices of all delirium subtypes. The ability of DOT to study pathophysiology and detect and monitor abnormalities could lead to an improvement in how we can investigate, diagnose, and prevent delirium. Additionally, we predict that the concurrent utilization of DOT with pharmacologic treatments, brain stimulation techniques, or other approaches in the future will open a new frontier for the clinical investigation of delirium. As for the research in the hospital, the device should have a good mobility and feasibility.

In this study, potential subjects will be recruited at the Tampa General Hospital by the psychiatry consultation-liaison team. Medical and surgical teams routinely place consult requests to the psychiatry team in order to seek assistance with the evaluation and management of delirious patients. Potential subjects will include such patients who have been determined to be delirious by the psychiatry team and if they do not violate the above stated inclusion/exclusion criteria. The consent process will take place in a private conference room or patient room in the Tampa General

Hospital. Only the Principal Investigator and Sub-investigator will obtain consent. The consent form will be thoroughly reviewed with the LAR and will only be signed after all questions have been asked and answered. The LAR will be reminded of legal rights prior to signing as well. Significant consent changes will result in reconsent.

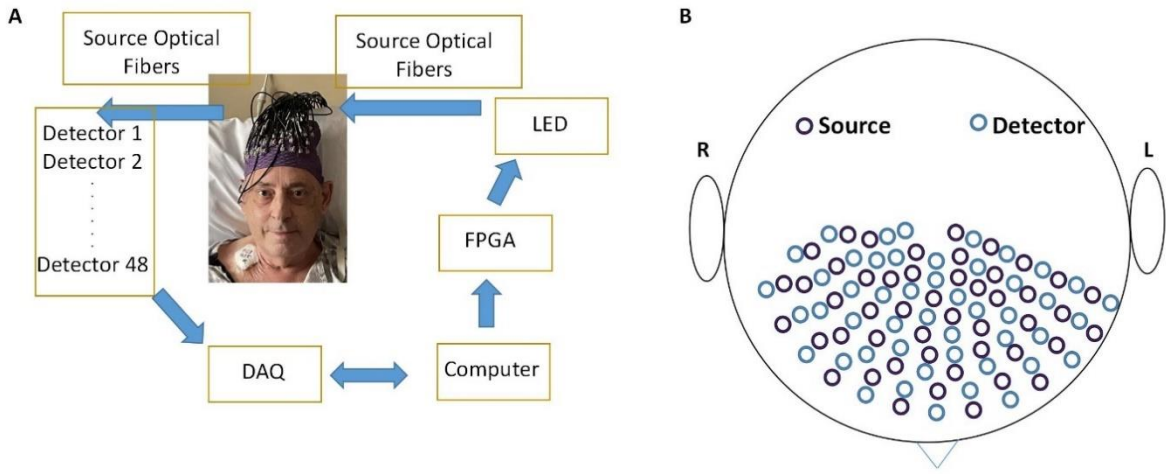

Figure 3.6 Schematic of portable DOT imaging system. A) Portable DOT imaging system hardware set up. B) Locations of the DOT sources and detectors over the brain surface. A total of 48 source-detector pairs placed on the prefrontal cortex.

3.7 Delirium Experiment

3.7.1 Experiment and Method

In the hospital study, the requirement of the imaging device should be cleaned and disinfected appropriately and transported around the hospital with a specially designed cart. The system consists of a main computer controlling groups of light emitting diodes via core boards which then deliver light beams in a timed sequence. The subsequent diffusing light is received by pairs of highly sensitive photodiode detectors (the DOT “probe”). This probe is connected to a two-layer interface coupled with a flexible electroencephalogram cap tailored to fit the head size of any subject.

In this experiment, 18 non-delirium subjects (9 men and 9 woman) with a mean age of 61.5 ± 5.2 years and 18 delirium patients (9 men and 9 woman) with 64.8 ± 7.2 years were initially recruited as paid volunteers. Two non-delirium subjects were excluded due to significant motion artifacts that could not be rectified. Three delirium subjects were excluded due to weak signal processing and volitionally leaving the experiment prior to completion of data collection. In total, 15 non-delirium individuals (8 men and 7 woman) with a mean age of 62.3 ± 6.7 years and 15 delirium individuals (8 men and 7 women) with a mean age of 69.1 ± 7.8 years were included for final analysis. All the participants were right-handed, and had normal or corrected-to-normal vision. All subjects were of Caucasian descent except for two Asian females (one from each study group).

During the imaging and data collection phase of the study, the device will be stored in the University of South Florida Psychiatry Consultation-Liaison office in the Tampa General Hospital. This is a secured room in an access-restricted building that uses no electronic entry methods. Only the principal investigator and attending physicians on the consultation-liaison service have keys that unlock this office (Tampa General Hospital security personnel possess such keys as well). When active imaging is being conducted, the device will be handled only by authorized study investigators trained to manage such equipment. The device will be transported around the hospital in a special cart designed by our lab. For longer-term storage after imaging is completed, the device will be stored in a secured room in an access-restricted building (The Department of Medical Engineering).

3.7.2 Hypothesis

The primary hypothesis in this study is to determine if diffuse optical tomography can be used to obtain resting-state and task-based functional neuroimaging information during and after

an episode of delirium. Secondary objectives include quantitatively correlating hemoglobin concentration alterations with delirium assessment scores and neuropsychological evaluations.

Our major hypothesis is that diffuse optical tomography will reliably capture hemodynamically based dysconnectivity and measure hemoglobin concentration derangements during an acute delirious episode, at rest and while performing a cognitive task. After resolution of the delirium, we anticipate that the subsequent quantitative analysis will result in an improvement of such functional data when compared to the acutely delirious state. Additionally, we hypothesize that the severity of delirium (as assessed by rating scales) will correlate with the measured changes in hemoglobin concentrations.

3.7.3 Data Acquisition and Withdrawal

For image acquisition, the DOT probe will be positioned over the bilateral dorsolateral prefrontal cortices as these are regions previously found to display high dysconnectivity in previous neuroimaging studies (as described in our background). A resting state scanning sequence will first be obtained for 5 minutes. Participants will be asked to let their minds wander, avoid repetitive thoughts, keep their eyes open, and maintain their attention on a central fixation point. This will be followed by an active task-based imaging sequence where the subject will be instructed to perform a Months Backwards test to focally activate the dorsolateral prefrontal cortices. Grading will be conducted on a 0 to 4 point scale and 30 seconds (if younger than 65 years old) or 60 seconds (over 65 years old) will be allowed for image capturing and test completion. The following anticipated circumstances will lead to acute withdrawal from the study:

First, the investigators consider it would be in the best interest of the subject (e.g., peripheral adverse event or onset of new clinically significant condition while assessment/imaging is being conducted).

Second, protocol violation which would increase risk of an adverse event to the subject. (e.g., hyperactive delirious subject becomes combative).

Third, subject's health care proxy or surrogate decides to withdraw consent for any reason. The subject and their health care proxy/surrogate will be contacted immediately to be notified of withdrawal. If this cannot be conducted on the first attempt, second and third attempts via telephone or in-person will be made. If subjects are withdrawn from the study before any imaging or assessments by our investigators are conducted, then any demographic/clinical characteristics data will be removed. If subjects are withdrawn after the first imaging set, but before the second data collection is conducted, then consent will be obtained from the health care proxy/surrogate for retention of the first data set.

3.7.4 Results and Conclusion

Hemodynamic activities were observed in the prefrontal cortex when participants were performing the Months Backwards verbal test. The preliminary results for this study consist of 4 healthy subjects and 4 delirious patients. As hypothesized, the quantitative hemodynamic response difference were reliably observed between healthy subjects and delirious patients in the bilateral prefrontal cortices. Data for control group and experiment group are shown in Figure 13,14 indicating the changes of [HbT], [HbO] and [Hb] during the Months Backwards verbal task. In Figures 13 and 14, the bold red,blue and yellow lines represent the average of [HbO], [HbT] and [Hb] for the 4 experiment trials. As illustrated, each trial generated a time-locked hemodynamic change accurately. In the control group, [HbO] and [HbT] began to increase sharply between 123-seconds to 125-seconds and peaked at 154-seconds. The peak value was calculated to be 3.36 μM and 0.74 μM for [HbO] and [HbT], respectively. [HbO] and [HbT] decreased sharply to the minimum level within 50 seconds after the 154-second, and returned to baseline in the next 10

seconds. As for the [Hb], it decreased sharply at 122-second point and reached the nadir at 156-second. The average value of change was calculated to be 2.62 μM.

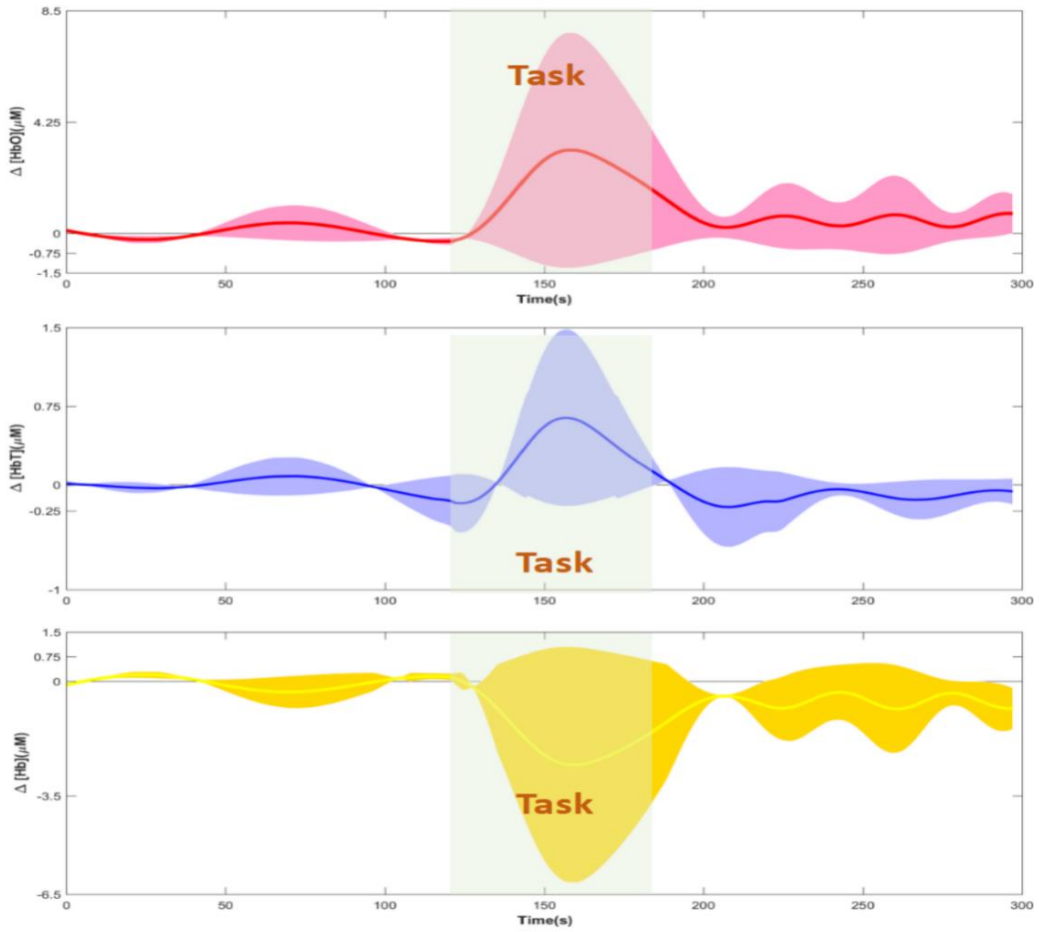

Figure 3.7 Hemodynamic response for healthy subjects' verbal test. Averaged time course of oxygenated [HbO], total [HbT], and deoxygenated [Hb] hemoglobin signals in the healthy subjects for the prefrontal cortex. The x-axis represents the time from 0 to 300s and the y-axis represents the mean and standard deviation for relative hemoglobin concentration in μM/L.

In the delirium experiment, a resting and tasking states scanning sequence will first be obtained for 5 minutes. In the first two minutes baseline resting status, participants were asked to let their minds wander, avoid repetitive thoughts, keep their eyes open, and maintain their attention on a central fixation point. Followed by an active task-based imaging sequence where the subject

will be instructed to perform a Months Backwards test to focally activate the dorsolateral prefrontal cortices, this status was marked as the tasking status, that has been represented in the green shadow in Figure 3.6 and 3.7. There are two groups delirium patient and non-delirium patient that have the same protocol during the Months Backwards test. Grading will be conducted on a 0 to 4 point scale and 30 seconds (if younger than 65 years old) or 60 seconds (over 65 years old) will be allowed for image capturing and test completion.

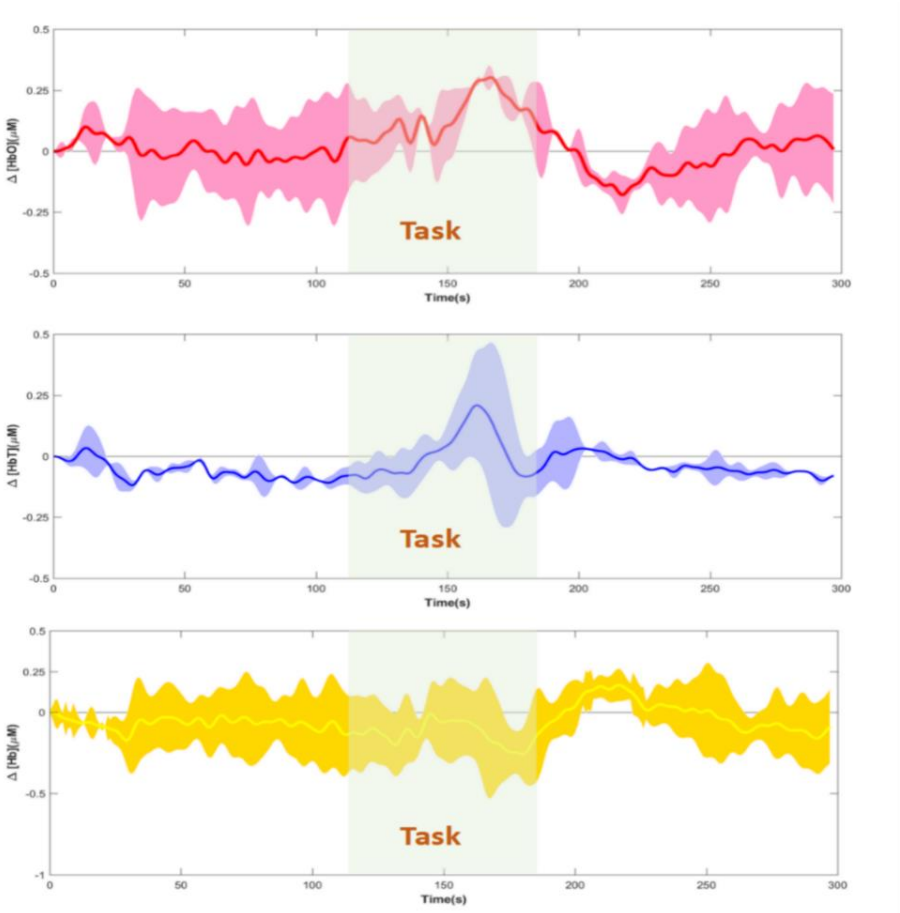

Figure 3.8 Hemodynamic response for delirium patients' verbal test. Averaged time course of oxygenated [HbO], total [HbT], and deoxygenated [Hb] hemoglobin signals in the delirium patients for the prefrontal cortex. The x-axis represents the time from 0 to 300s and the y-axis represents the mean and standard deviation for relative hemoglobin concentration in μM/L.

In the delirium group, [HbO] and [HbT] increased more gradually and their values plateaued in comparison to the healthy subjects at 161-second. The average values of hemoglobin change in this group were started to be decreased at 0.26 μM and 0.24 μM for [HbO] and [HbT], respectively. [Hb], in a similar fashion, decreased gradually and reached a nadir later at 177-second point and the value of change was calculated to be 0.24 μM.

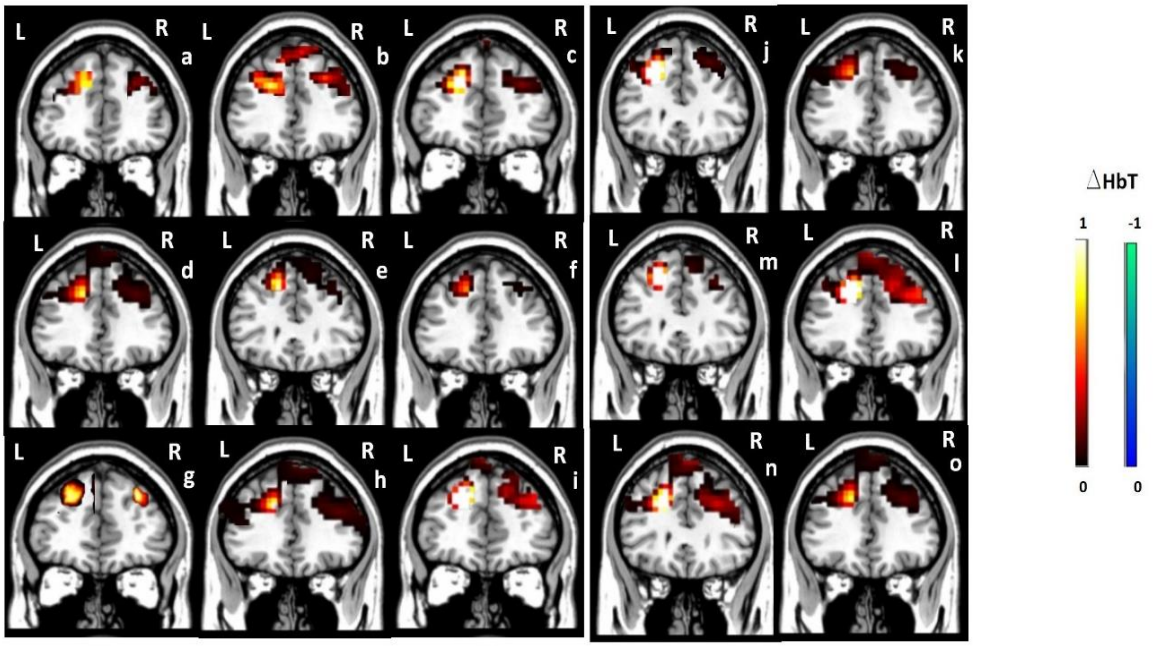

Figure 3.9 Image reconstruction for non-delirium subjects at HbT peak value time point. Non-delirium subjects #1-#15 of frontal section of HbT images at HbT peak value time point (a-o) in prefrontal cortex.

Those 15 DOT images shown in Figure 3.9 and 3.10 presents the brain activation during the Month Backwards Test experiment. The cognitive verb test is wildly used in the neuropsychiatric disorder evaluation especially in the delirium prediction. In this study, we captured the time point at the HbT peak value time point in order to compare the peak brain activation between delirium patients and non-delirium patients.

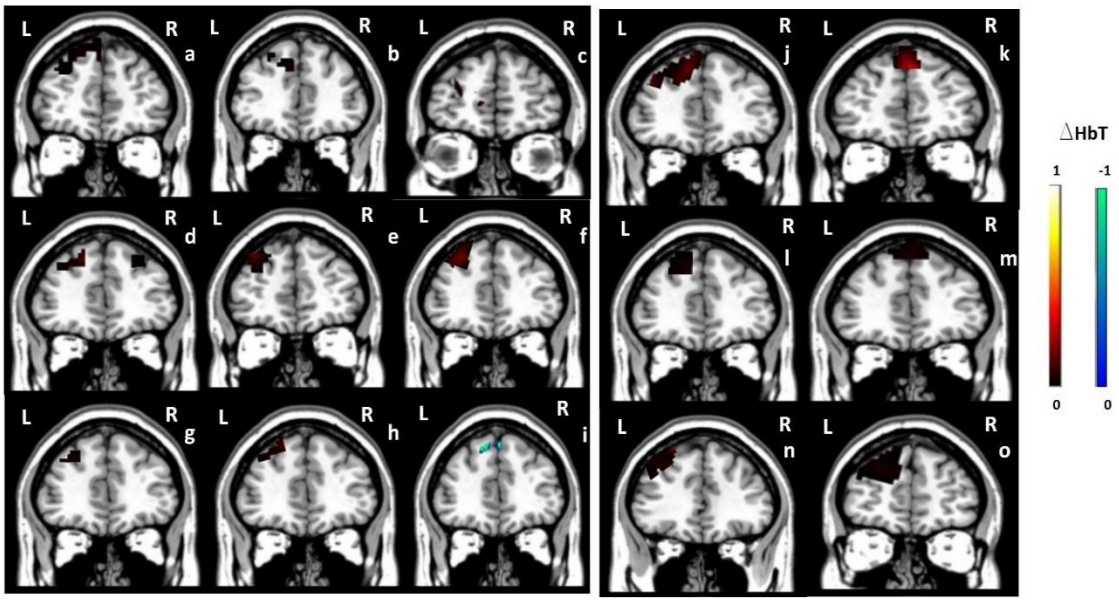

Figure 3.10 Image reconstruction for delirium patients at HbT peak value time point. Delirium subjects #1-#15 of frontal section of HbT images at HbT peak value time point (a-o) in prefrontal cortex.

The three-dimensional functional imaging was successfully captured by our portable DOT imaging system. In the provided coronal view of prefrontal cortex, clear distinction in activation patterns between non-delirium and delirium subject can be observed. Non-delirium subjects were observed to have a more robust area of activation compared to the baseline. In comparison, the delirium individuals had a weak change and activation in hemodynamic response with a restricted distribution pattern.

In this preliminary study, we demonstrate the ability of a novel DOT system to capture cerebral hemodynamic activity in delirious and healthy individuals. As our study continues, we plan to further enroll subjects to increase our sample sizes, conduct a functional connectivity analysis to study any dysregulation that may occur within the prefrontal cortex or other regions of the brain, and conduct formal statistical analyses.

In addition, the obstacles regarding the DOT setup itself in the future should be mentioned. Due to the physical limitations of the optical fibers and optodes used in the portable DOT system design, meticulous planning of the array must be considered. Movement artifacts, as with any other techniques, is still a significant barrier that will inevitably be presented [11]. The construction of the optical fiber optodes with fixation may help reduce the possibility of this phenomenon, along with further advancements in post processing and filtering methodologies. Physiological signal contamination is another technical limitation that is common to all optical methods especially. Although DOT suffers much less from scalp interference (compared to fNIRS), the presence of hair itself or dark shades have a big influence on signal quality. As such, the pinning or separation of hair is a moderate and imprecise method often employed. Further development of analysis and filtering algorithms may assist with bypassing this issue. Lastly, the maximum depth that can be reliably and accurately imaged is greater than fNIRS, though is still limited compared to fMRI [10]. It is estimated to be approximately 5 cm, which reduces the ability to detect deeper brain structures, but more than capable of capturing cortical and some subcortical structures [11].

3.8 References

1. Huang, Jingyu et al. Three-dimensional Optical Imaging of Brain Activation During Transcranial Magnetic Stimulation. *Journal of X-ray science and technology*. 2021 Jan: 891 – 902.

2. Dai X, Zhang T, Yang H, Tang J, Carney PR, Jiang H. Fast noninvasive functional diffuse optical tomography for brain imaging. *J. Biophotonics*. 2017; e201600267.

3. Barut C, Kızıltan E, Gelir E, Köktürk F. Advanced analysis of finger-tapping performance: a preliminary study. *Balkan Med J*. 2013 Jun;30(2):167-71.

4. Suzanne T. Witt, Angela R. Laird, M. Elizabeth Meyerand. Functional neuroimaging correlates of finger-tapping task variations: An ALE meta-analysis. *NeuroImage*, Volume 42, Issue 1, 2008, Pages 343-356, ISSN 1053-8119.

5. Turesky TK, Olulade OA, Luetje MM, Eden GF. An fMRI study of finger tapping in children and adults. *Hum Brain Mapp*. 2018 Aug;39(8):3203-3215.

6. Nitchingham A, Kumar V, Shenkin S, Ferguson KJ, Caplan GA. A systematic review of neuroimaging in delirium: predictors, correlates and consequences. *Int J Geriatr Psychiatry*. 2018 Nov;33(11):1458-1478

7. Haggstrom L, Welschinger R, Caplan GA. Functional neuroimaging offers insights into delirium pathophysiology: A systematic review. *Australas J Ageing*. 2017 Sep;36(3):186-192

8. Choi SH, Lee H, Chung TS, Park KM, Jung YC, Kim SI, Kim JJ. Neural network functional connectivity during and after an episode of delirium. *Am J Psychiatry*. 2012 May;169(5):498-507

9. Hoshi Y, Yamada Y. Overview of diffuse optical tomography and its clinical applications. *J Biomed Opt.* 2016 Sep;21(9):091312

10. Jiang H *et al*. Diffuse Optical Tomography: Principles and Applications. CRC Press, 2010.

11. Jiang, S., Huang, J., Yang, H. *et al.* Neuroimaging of depression with diffuse optical tomography during repetitive transcranial magnetic stimulation. *Sci Rep* volume 11, 7328 (2021).

Chapter 4: Significance and Specific Aims of the Research

4.1 Public Health Relevance of the Research

Mental health and suicide are events that are unfortunately has become more common over the past decades. Mental illness and symptoms are probably always the equation when assessing death by suicide. However, the mechanism for major mental illness is unclear. The Brain imaging has proven offering valuable information regarding the unanswered questions. Because of the immediate brain change happening, few modalities possess the temporal resolution can be captured. Major depressive disorder and delirium are mental health illness lined to significant functional impairment and mortality. It is the primary and the most common mental disorders in the United States. For the major depressive disorder, an estimated 17.3 million adults had at least one major depressive that significantly diminishes psychosocial functioning and overall quality of life. Depression would last for midlife or beyond. Some serious medical illnesses, such as diabetes, cancer, lung disease, heart disease, and Parkinson's disease would be the reason to generate the depression. Current research suggests that depression is caused by a combination of genetic, biological, environmental, and psychological factors.

Delirium is a syndrome of acute brain failure that represents a change from an individual's baseline cognitive functioning, characterized by deficits in attention, awareness, and multiple aspects of cognition that fluctuate in severity over time. It is the most common neuropsychiatric disorder observed in hospitalized patients [1]. The incidence of delirium ranges from 11% to 42% [2] and can be as high as 87% among critically ill patients [3]. It is associated with increased mortality, rate of complications, hospital length of stay, and institutionalization after discharge [4-

6]. The estimated health care cost of delirium in the United States is $150 billion per year [7]. Despite how prevalent and potentially life-threatening this syndrome is, little is known about its underlying specific mechanisms.

4.2 Scientific Premise of the Research

Optical imaging has been used for decades in the literature with no reported significant health risks or hazards. The known theoretical risks include tissue damage from heating and blindness due to direct light exposure to the eyes. These risks, however, are minimal to none. Regarding the first possible risk, the optical power that will be used during these procedures is insufficient to cause tissue heating. In our system, the maximum power from the light source (light-emitting diodes) is approximately 0.5 mJ/cm^2, which is significantly lower than the safety standard of 20 mJ/cm^2 (per the American National Standard for Safe Use of Lasers). In fact, if the power exceeds 0.5 mJ/cm^2, the light source would be subsequently damaged, thus self-discontinue the procedure and inherently prevent any risk of overheating the tissue. In terms of the risk of blindness, this is also extraordinarily minimal because the light will be delivered to the head through specially designed enclosed optic fibers. Additionally, to further eliminate the risk of blindness participants will be asked to wear optical protective goggles.

The interest of area in this study would be located in the prefrontal cortex, because the prefrontal cortex plays an important role in the cognitive control functions. In the TMS and depression study, the left DLPFC is the most common target for treating depression not only necessarily due to this specific region itself, but from studies demonstrating that it modulates the blood flow response and activity of the anterior cingulate cortex as well. The rates of perfusion and metabolism in this region in particular may predict response to treatments. Thus, our depth analyses may demonstrate that either our treatment parameters were not adequate enough to

generate appropriate activation or again, that depressed individuals at baseline have reduced hemodynamic responses in the future.

In the depression study, although, the FDA approved parameters combination can be selected as the treatment protocol in the clinical depression treatment, ideal stimulation parameters have remained unknown as there has previously been no reliable mechanism to measure neural connectivity and responses in real time [8]. Utilizing DOT simultaneously with TMS in testing variable frequencies, intensities, number of pulses, and interval timings offers a new promising approach to allowing such exploration in real time and with three dimensional images. Cortical activation/inhibition patterns and hemodynamic responses would be reliably captured in healthy individuals.

4.3 Technological Significance of the Research

As the development of neuroimaging in neuropsychiatric disorders, nowadays, it offers the possibility of probing the mechanisms and networks involved in delirium. Imaging can be used to quantify normal or pathological physiology, localize abnormalities to specific brain regions, and offer objective information for diagnostic, preventative, and treatment purposes. Functional techniques particularly may be able to elucidate our understanding of cerebral hemodynamic activity during and after delirium [9]. Previous neuroimaging studies in delirium have utilized modalities such as near-infrared spectroscopy, functional magnetic resonance imaging, single photon emission computed tomography, positron emission tomography, and transcranial doppler [10]. One of the most pertinent findings reported thus far is significant network dysfunction of the dorsolateral prefrontal cortex and posterior cingulate cortex. Overall though, significant limitations of these techniques and their studies exist and include poor spatial resolution, cost and feasibility, portability, hypoactive subtypes only, and a lack of task-based protocols.

As such, we have developed a novel portable DOT device to be used for the study of delirium. DOT is an emerging technique that is based on near-infrared light and is able to reliably capture brain activity via hemoglobin concentration assessments as our surrogate markers of activation. We propose to use DOT to capture images of resting state and task-based neural activity in the prefrontal cortices of all delirium sub-types. The ability of DOT to study pathophysiology and detect and monitor abnormalities could lead to an improvement in how we can investigate, diagnose, and prevent delirium [11]. Additionally, we predict that the concurrent utilization of DOT with pharmacologic treatments, brain stimulation techniques, or other approaches in the future will open a new frontier for the investigation of delirium in the hospital. In this study, we propose to apply DOT to delirious subjects and evaluate and test whether diffuse optical tomography can provide brain activation and functional connectivity data during and after an episode of acute delirium. In future work, we will focus on further studying underlying neurobiological mechanisms of delirium with DOT.

4.4 Specific Aims

4.4.1 Aim 1

This aim is concerned with demonstrating the capabilities of DOT in human brain imaging during the TMS stimulation. This aim is basic, and it must do for the experimental and instrumentation of this research. The hypothesis of this study is that optical methods coupled with model-based image formation from tomographically-measured optical data provides brain activation and connectivity during transcranial magnetic stimulation on patients experiencing depression disorder. The primary objective of this study is to determine if DOT is able to offer quantitative information to detect the effect of transcranial magnetic stimulation on depression patients and optimize the parameters of transcranial magnetic stimulation. To better image the

brain cortical structures associated with the functional activities like oxygen saturation by DOT, enough optical energy should be delivered to the tissue [12]. To achieve this aim, firstly, we tested our prototype system for light delivery/detection to the changed conditions in a clinical setting. After this system has been tested, we recruited the healthy subject as control to evaluate the system in the clinical environment. In previous studies, it is already stated that the light absorption by tissue depends on the wavelength. As for NIR wavelength, the optical absorption coefficient of the skull is higher at $\lambda < 700n$m, while it is relatively lower at $700nm < \lambda < 1000n$m. The optical absorption of cortical issue include blood vessels also varies in this wavelength range [13]. After evaluating and optimizing the TMS experiment produce for several trials, we can iterate our designs to perfect the clinical operation for subsequent experiment.

4.4.2 Aim 2

Aim 2 is concerned with developing and testing the efficacy of a novel diffuse optical tomography imaging guided system for healthy subject and delirium patient. This aim evaluates the feasible and convenient features for the clinical and hospital utilization. Before collecting data from the delirium patient, we need to evaluate whether the new diffuse optical tomography can provide brain activation and functional connectivity data during the for healthy subjects in the verbal test. In this study, five healthy subjects were enrolled in the study. During the experiment, one minute month backwards test come after two minutes resting time in the beginning. After one minute month backwards test, the participant enters into another two minutes resting time. The experiment exists 5 minutes in total. In this study, we need to find the difference of hemodynamic activation between healthy subject and delirium patient. This work can demonstrate and verify whether the new fast DOT system has the potential to become a powerful tool for noninvasive three-dimensional imaging of the brain. With the observation of hemodynamic response for the

healthy subject and delirium patient by DOT, we can determine whether DOT is able to offer quantitative information to detect the verbal test stimulation on delirium patients and help the doctor to judge how serious of the delirium patients are.

4.5 References

1. Maldonado JR. *et al*. Acute Brain Failure: Pathophysiology, Diagnosis, Management, and Sequelae of Delirium. *Crit Care Clin*. 2017 Jul;33(3):461-519.

2. Siddiqi N, House AO, Holmes JD. Occurrence and outcome of delirium in medical in-patients: a systematic literature review. *Age Ageing*. 2006 Jul;35(4):350-64.

3. Gilchrist NA, Asoh I, Greenberg B. Atypical antipsychotics for the treatment of ICU delirium. *J Intensive Care Med*. 2012 Nov-Dec;27(6):354-61.

4. Inouye SK. Delirium in older persons. *N Engl J Med*. 2006 Mar 16;354(11):1157-65.

5. McCusker J, Cole M, Abrahamowicz M, Primeau F, Belzile E. Delirium predicts 12-month mortality. *Arch Intern Med*. 2002 Feb 25;162(4):457-63.

6. Kakuma R, du Fort GG, Arsenault L, Perrault A, Platt RW, Monette J, Moride Y, Wolfson C. Delirium in older emergency department patients discharged home: effect on survival. *J Am Geriatr Soc*. 2003 Apr;51(4):443-50.

7. Inouye SK, Westendorp RG, Saczynski JS. Delirium in elderly people. *Lancet*. 2014;383(9920):911–922.

8. Jiang S, Huang J, Yang, H. *et al.* Neuroimaging of depression with diffuse optical tomography during repetitive transcranial magnetic stimulation. *Sci Rep* volume 11, 7328 (2021).

9. Andrew R. Mayer, Davin K. Quinn, Neuroimaging Biomarkers of New-Onset Psychiatric Disorders Following Traumatic Brain Injury. *Biological Psychiatry*, 10.1016/j.biopsych.2021.06.005, 91, 5, (459-469), (2022).

10. Jonathon P. Fanning, Samuel F. Huth, Chiara Robba, Stuart M. Grieve, David Highton, Advances in Neuroimaging and Monitoring to Defend Cerebral Perfusion in Noncardiac Surgery. *Anesthesiology* 2022; 136:1015–1038.

11. Wilson, J.E., Mart, M.F., Cunningham, C. *et al.* Delirium. *Nat Rev Dis Primers* volume 6, 90 (2020).

12. Qingguang Z, Kyle W Gheres, Patrick J D, Origins of 1/f-like tissue oxygenation fluctuations in the murine cortex. *Plos Biology*, July 15, 202.

13. Konstantin Maslov, Hao F Zhang and Lihong V Wang. Effects of wavelength-dependent fluence attenuation on the noninvasive photoacoustic imaging of hemoglobin oxygen saturation in subcutaneous vasculature in vivo. *IOP Science,* November 2007.

Chapter 5: Manuscripts[1]

This chapter contains two manuscripts based on this research: - (5.1, 5.2). A Third and fourth manuscript are in progress. 5.1, titled "Three-dimensional optical imaging of brain activation during transcranial magnetic stimulation" is published in Journal of X-Ray Science and Technology. Permission is included in appendix B. It is based on the application of the structural and functional imaging capabilities of diffuse optical tomography imaging to study brain activities during the TMS stimulation for healthy subjects. I am the first author in this paper. The paper appears here in the original form in which it was written.

The second manuscript, 5.2 is titled "Neuroimaging of depression with diffuse optical tomography during repetitive transcranial magnetic stimulation**"** is published in Scientific Report. Permission is included in appendix B. This paper talks about the difference between brain activation and hemoglobin response between healthy group and depressed patient group. I am the co-first author in this paper. The paper appears here in the original form in which it was written. In this published paper, we tried to find the correlation between level of depression and hemodynamic response. We hypothesized that the depressed patients would not as sensitive as the healthy subjects. In this study, the brain activities were monitored by our DOT imaging system for both healthy and depressed patient groups. With the same level of TMS stimulation, we can compare the results and evaluate the depressed level. In the future, our results for the depressed

[1] This chapter contains two sections. The first section, 5.1, was published in The Journal of X-ray Science and Technology. The second section, 5.2, was published in Scientific Report. Permission is included in Appendix B.

patient can be correlated by the level of depression, that can help the doctor evaluate the effective of the TMS treatment.

5.1 Three-dimensional Optical Imaging of Brain Activation During Transcranial Magnetic Stimulation[2]

5.1.1 Abstract

Repetitive transcranial magnetic stimulation (rTMS) to the left prefrontal cortex with 10 Hz is a common clinical protocol for major depressive disorder (MDD). Noninvasive neuroimaging during rTMS allows to visualize the cortical brain activation and response, and to optimize treatment parameters for rTMS. In this paper, we present a fast diffuse optical tomography (DOT) approach for three-dimensional brain mapping of hemodynamics during rTMS. Ten healthy subjects were enrolled to the study. These subjects received the 10 Hz stimulation with 80% and 100% resting motor threshold (rMT), respectively, in 4 seconds for each stimulation. Significant hemodynamic activation was observed in all cases with the strongest response when 100% rMT stimulation was applied. This work demonstrates that fast DOT has the potential to become a powerful tool for noninvasive three-dimensional imaging of the brain during rTMS.

5.1.2 Introduction

Repetitive transcranial magnetic stimulation (rTMS) is a non-pharmacological, non-invasive brain stimulation technique which is used for various psychiatric disorders. Though studied the most for major depressive disorder, its use in schizophrenia, posttraumatic stress disorder, substance use disorders, and obsessive-compulsive disorder is also being investigated.

[2] The section 5.1 was published in The Journal of X-ray Science and Technology. Jingyu Huang is the only first author for this paper. Shixie Jiang, Hao Yang corrected the English. Ryan Wagoner, F Andrew Kozel, Gleen Currier are doctors and help recruited the subjects in the clinical study. Huabei Jiang is the telecommunication author. Permission is included in Appendix B.

Despite ongoing research, our knowledge of the underlying mechanism of TMS is poorly understood. While rTMS is effective for psychiatric disorders treatment, different antidepressant effect has been reported through the stimulation of left dorsolateral prefrontal cortex (DLPFC) by different field intensity, number of stimuli per session and the number of treatments, and the activation mechanism is largely unclear [1]. To better understand the brain activation areas associated with rTMS, several neuroimaging modalities such as single-photon emission computerized tomography (SPECT), positron emission tomography (PET), and functional magnetic resonance imaging (fMRI) have been used to image the brain during TMS [2]. However, these imaging techniques have not shown their utility for brain imaging during rTMS, due to their low temporal resolution along with other limitations such as the cost,

Electroencephalography (EEG), magnetoencephalography (MEG), and functional near-infrared spectroscopy (fNIRS) are fast techniques and have also been used for brain mapping during rTMS [3]. However, these techniques have very low spatial resolution, and thus their utility for brain imaging during rTMS is also limited. Although fNIRS has no electromagnetic interference and possess portable, cost-effective, and noninvasive, little and shadow depth information can be presented out and it does not have a very good penetration which could not dig out much brain activation during the rTMS stimulation. As for the functional magnetic resonance imaging (fMRI) and diffusion tensor imaging (DTI) use signals that involve the electromagnetic spectrum, the resolution and the image quality would be influenced by significant measurement artifacts, because the TMS coil produces series of very strong magnetic and electrical fields. Diffuse optical tomography (DOT) is an emerging neuroimaging modality that is based on near-infrared (NIR) optical technologies and model-based inverse computations [4]. It can be considered as an extension of fNIRS, but DOT is able to provide three-dimensional images of

hemoglobin and blood volume/oxygenation with centimeter scale resolution. In addition, like fNIRS, DOT measures functional brain changes without using electrical or magnetic signals, and thus, there are no electromagnetic interactions between DOT and rTMS. Here we report a first-in-human study applying this combination DOT and rTMS in human study.

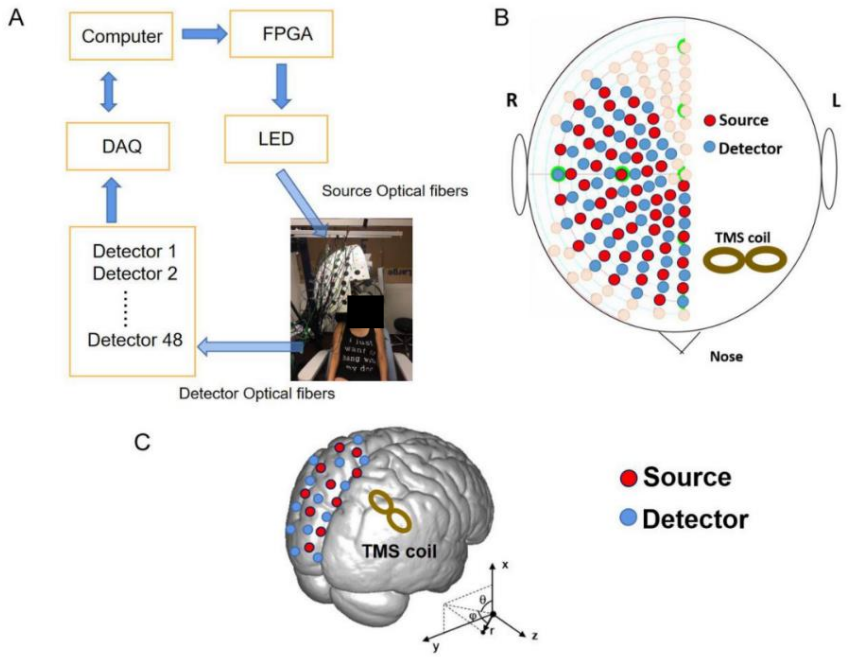

Figure 5.1 Schematic of DOT brain imaging system. A) Schematic of the DOT system. B) Locations of the rTMS coil and the DOT sources and detectors over the brain. A total of 48 source-detector pairs placed on the right hemisphere. C) Schematic of 3D location of rTMS coil and DOT sources and detectors.

5.1.3 Materials and Methods

5.1.3.1 Subjects

In this experiment, eight healthy subjects (7 men and 1 woman) with a mean age of 33.5 ± 15.9 years were recruited as paid volunteers. Three healthy subjects were excluded because of significant motion artifacts and discontinuous signal. As a result, 5 healthy subjects (4 men and 1

woman) with mean age of 36.9 ± 11.8 were included for final analysis. All of the participants were right-handed, as determined by the modified Edinburgh Handedness Questionnaire (Oldfield 1971), and had a normal or corrected-to-normal vision. The potential neurological or psychiatric disorders were excluded. The study protocol was approved by the University of South Florida Institutional Review Board. Written informed consent was obtained from all the participants.

5.1.3.2 TMS and DOT Procedures

Participants were positioned in the TMS device chair and adjusted to ensure comfort throughout the experimental procedure. Ear plugs were inserted in order to decrease the impact of hearing upset from the noise of TMS machine. All external light was blocked from entering the clinical room, and the ambient lighting was tested to ensure that it did not contaminate the DOT signal. The DOT probe consisting of 48 sources and 48 detectors was then positioned over the region of the right prefrontal cortex. The DOT is a contralateral measurement over the region on the right prefrontal cortex while the TMS stimulation start on the left prefrontal cortex. Optical probes covered the entire contralateral dorsolateral prefrontal cortex (DLPFC), which can monitor the major part of DLPFC. The probes were fastened using Velcro straps and attached against the scalp with their tips directly touching the skin for maximum efficiency of light transmission. The hair strands under the probe were manually moved away using combs to facilitate optimal contact. This helped avoid potential contamination by light absorption in hair.

The rTMS was performed using a Neuronetics' NeuroStar system. One hertz TMS pulse with 45% of device output was delivered to the left cortex in order to locate the estimated motor strip by observing the muscle twitch of the abductor pollicis brevis in the right hand [5]. After several re-positioning the TMS coil and reliable muscle twitch observed, we located and marked the motor cortex area. The motor threshold (MT) is defined as the lowest level of stimulation capable of causing a twitch in the contralateral thumb by TMS motor threshold assessment tool

[6]. According to the TMS protocol, the location of TMS stimulation was defined as 5 cm anterior to the motor cortex position in a para-sagittal line. Stimulation with 80% and 100% resting motor threshold (rMT) was, respectively, applied during the experiment. The participants were instructed to sit quietly with eyes open, stay awake, and not move. DOT data were acquired 1.5 min prior to the stimulation, during the 24 stimulation/rest epochs (30 s per epoch), and during another 1.5 minutes post-stimulation period, resulting in a total recording time of 15 minutes. The resting gap between the two consecutive experiments was 5 minutes. The stimulation epochs consisted of 4 s of 10 Hz stimulation and 26 s of rest, and were repeated 24 times for each experiment. A 90 second baseline was recorded respectively before each TMS stimulation experiment in different rMT stimulation.

5.1.3.3 Diffuse Optical Tomography System and Image Reconstruction

Diffuse optical tomography (DOT) is a noninvasive imaging technique that exploits the relative transparency of biological tissue to near-infrared (NIR) light (600~950 nm). As the near-infrared wavelength range between roughly 600 and 950 nm is poorly absorbed relatively by biological tissue, light can travel through up to several centimeters of tissue because of low intrinsic optical absorption of biological tissue. In this range of light spectrum, most biological tissue have low absorption, however, oxy-hemoglobin and deoxy-hemoglobin are the major absorbers. Thus, this two spectrum we used (780nm and 850 nm) is ideally suited for monitoring the changes, which can achieve a high signal-to-noise level relatively [9]. Over the past 15 years, diffuse of tomography has been successfully utilized in imaging epilepsy, breast cancer, osteoarthritis, and cortical activation [10]. It has been proved that DOT has the ability to monitor hemodynamic activity in terms of spatial resolution (around 5cm penetration) compared to fMRI. Moreover, it is portable, noninvasive, safe and cost-effective.

We used a fast multispectral DOT system for optical signal recording, as described in detail previously [8,11]. The system performs continuous-wave (CW) measurements using 48 light-emitting diodes (LEDs) as the excitation sources and highly sensitive photodetectors as the light detectors. Forty-eight optical source/detector pairs were distributed over the right hemisphere of the brain and attached firmly to the scalp. The average distance between 2 adjacent source-detector positions was nearly 1 cm. The sources/detectors were also attached to a two-layer interface coupled with a 256-channel medium size EEG cap which fits all the head sizes of the participants in this study. Tomographic optical data were collected this with a temporal resolution of 14.4 Hz at two NIR wavelengths (780 and 850 nm). The row optical data from all channels were inspected to exclude the epochs with significant discontinuity due to the motion artifacts during the measurement. After excluding the suspected 'discontinuous channel', a blackmanharris window-based finite impulse response filter was applied to remove the instrumental noise.

The three-dimensional (3D) images of tissue absorption coefficient were reconstructed using a finite element method (FEM)-based inverse algorithm, as described in detail previously. The 3D finite element mesh for each brain was produced using the brain contour measured a 3D magnetic space digitizer coupled with a head atlas approach [12]. And the three-dimensional (3D) images of tissue absorption coefficient were reconstructed using a finite element method (FEM)-based inverse algorithm [13,14,15]. The FEM-based algorithm allows the recovery of tissue absorption coefficient in 3D based on an iterative regularized Newton method [16], and the concentrations of oxy- and deoxy-hemoglobin ([HbO] and [Hb]) were then calculated using the recovered absorption coefficients at both wavelengths based on the Beer-Lambert law [17]. Coupled with a least-square fitting procedure and pseudo inverse matrix calculation, hemoglobin

concentration, [HbT], was calculated by summing up [HbO] and [Hb] which is proportional to cerebral blood volume (CBV).

5.1.4 Statistical Analysis

Data analysis was conducted using MATLAB (version R 2018a) and SAS (9.4). All the epochs (the 30s) in the session were averaged for each channel and the data are shown as the mean ± standard deviation. We used a paired Student's t-test for comparison of means. All statistical analysis were performed at a significance level of 0.05. Data before and after the rTMS treatment were analyzed with two-tailed paired t-tests. Subject means were allowed to vary around an individualized intercept across trials with stimulation type as a within-subject factor. Redundant analysis was conducted using repeated measures analysis of variance (ANOVA) to allow an appropriate interpretation of the results.

5.1.5 Results

As hypothesized, there was an observable difference in the heodynamic response between 80%rMT and 100% rMT stimulation within the right dorsolateral prefrontal cortex. Averaged HbT for the subjects over time under 80% rMT stimulation is shown in Figure 5.2, indicating the dynamic change of [HbT] during the total 24 trials of TMS stimulation (each trial consisted of 4 seconds of TMS stimulation state and 26 seconds of resting state). The blue bold line represents the averaged [HbT] for the 24 trials. The other 5 plots indicate the individual time curves for different healthy subject which show a similar hemodynamic change compared to each other. We note that each trial of TMS stimulation generated a time-locked hemodynamic change in the right prefrontal cortex. The increase of [HbT] started right after the TMS pulse was delivered, reached the peak around the 8^{th} to 12^{th} second, and then decreased slowly after the peak. As for 100% rMT stimulation, we see that the [HbT] increased right upon the onset of TMS stimulation and reached

its peak at around the 9th to 14th second followed with continued decrease afterwards. The average absolute value for [HbT] change was calculated to be 1.52 uM at 9.3 second for 80% rMT and 3.45 uM at 10.24 second for 100% rMT.($P<0.01$, t test, [HbT])

When comparing the two groups, as many studies showed that the hemodynamic response (HR) to brief neural activity caused by the blood oxygen level-dependent effect is delayed some seconds, and the HR latency varies among activation sites, especially since this is in response to repetitive stimulation [18]. On the other hand, the average absolute peak [HbT] with different rMT stimulation occurred around 10 second and then decreased gradually. There was a significant difference in the [HbO] and [HbT] response between 80% rMT and 100% rMT stimulation. In general, the response to 100% rTM stimulation was higher than 80% rTM for all the subjects.

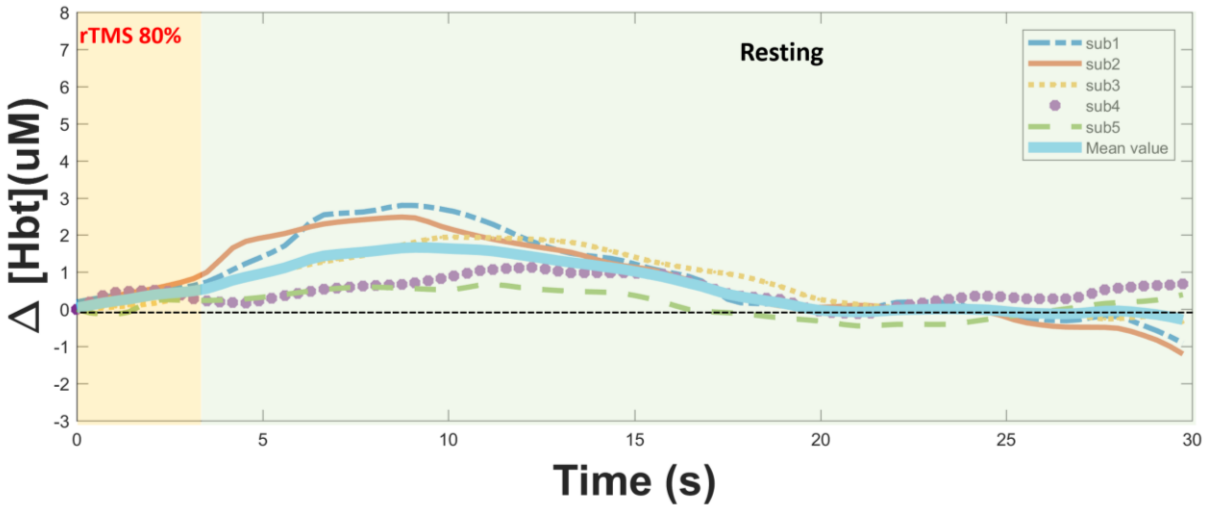

Figure 5.2 Healthy subjects' HbT hemodynamic response during 80% MT TMS stimulation. Time course of averaged total hemoglobin (HbT) for all the subjects under 80% rMT stimulation in the prefrontal cortex. Ten hertz stimulation was performed for 4 s followed by 26 s of rest for 12 epochs. The x-axis represents the time from 0 to 30 s in the epoch, and the y-axis represents the mean and 95% confidence interval of HbT concentration in μM/L.

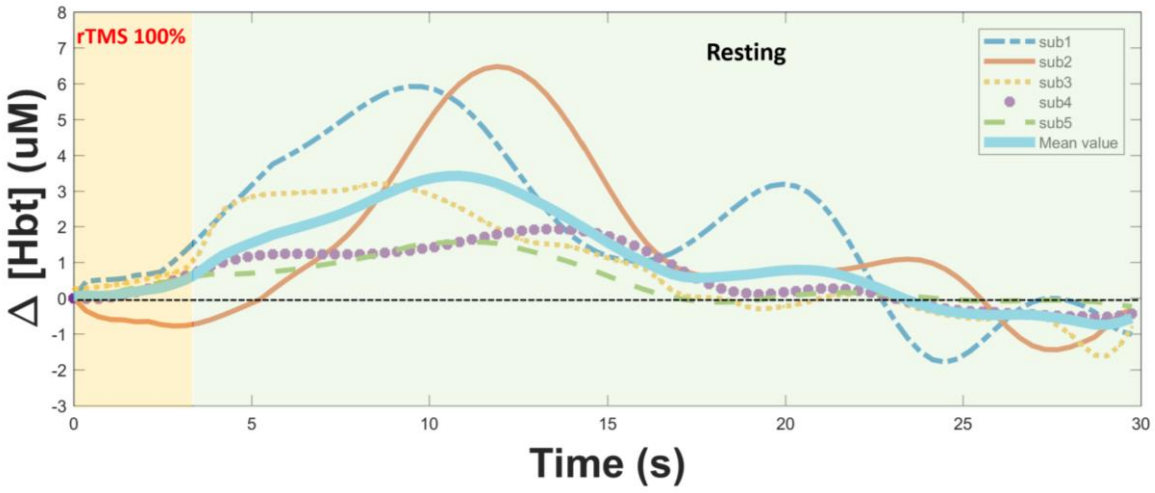

Figure 5.3 Healthy subjects' HbT hemodynamic response during 100% MT TMS stimulation. Time course of averaged total hemoglobin (HbT) for all the subjects under 100% rMT stimulation in the prefrontal cortex. Ten hertz stimulation was performed for 4 s followed by 26 s of rest for 12 epochs. The x-axis represents the time from 0 to 30 s in the epoch, and the y-axis represents the mean and 95% confidence interval of HbT concentration in μM/L.

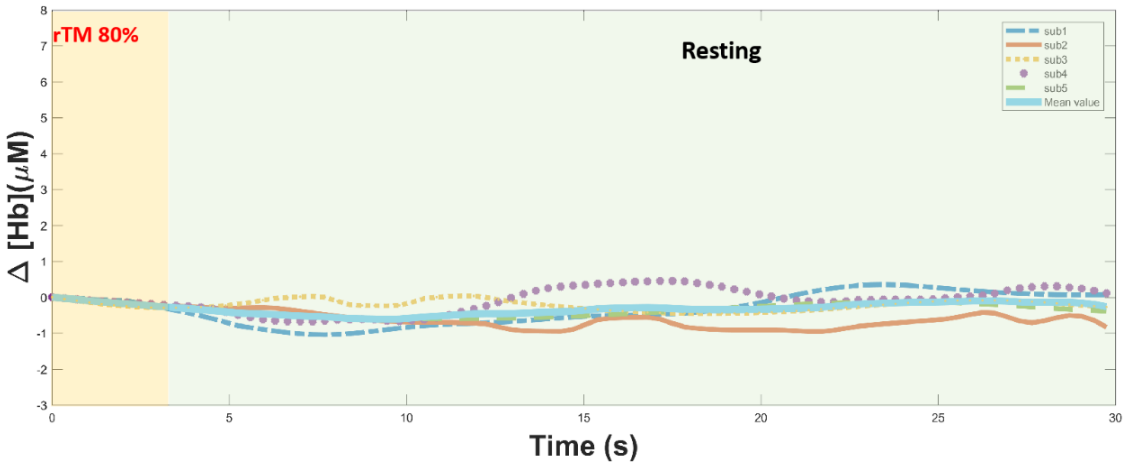

Figure 5.4. Healthy subjects' Hb hemodynamic response during 80% MT TMS stimulation. Time course of averaged deoxy-hemoglobin (Hb) for all the subjects under 80% rMT stimulation in the prefrontal cortex. Ten hertz stimulation was performed for 4 s followed by 26 s of rest for 24 epochs. The x-axis represents the time from 0 to 30 s in the epoch, and the y-axis represents the value of Hb concentration in μM/L.

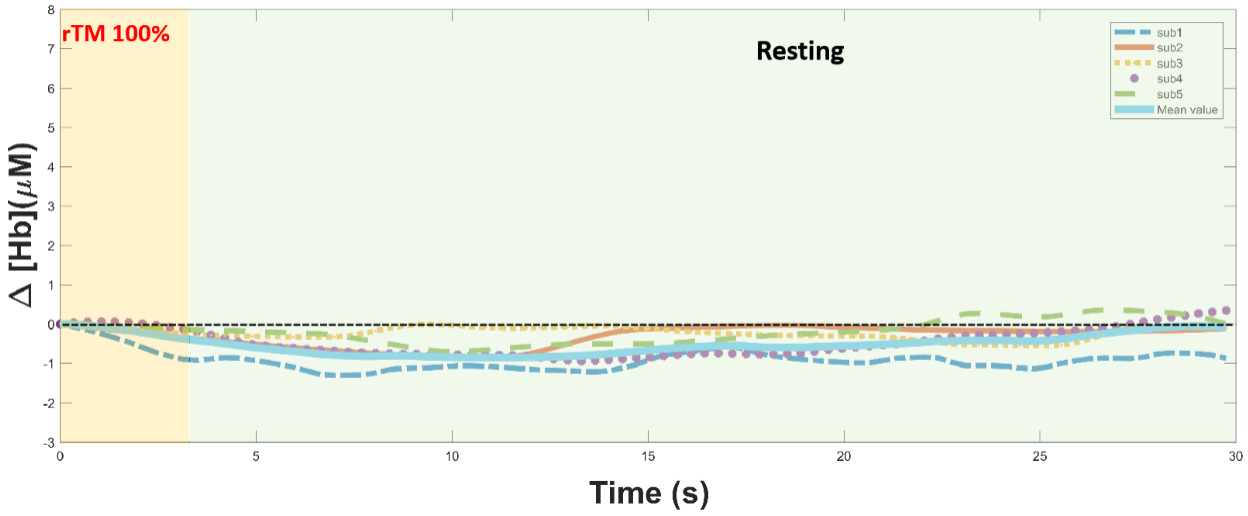

Figure 5.5. Healthy subjects' Hb hemodynamic response during 100% MT TMS stimulation. Time course of averaged deoxy-hemoglobin (Hb) for all the subjects under 100% rMT stimulation in the prefrontal cortex. Ten hertz stimulation was performed for 4 s followed by 26 s of rest for 24 epochs. The x-axis represents the time from 0 to 30 s in the epoch, and the y-axis represents the value of Hb concentration in μM/L.

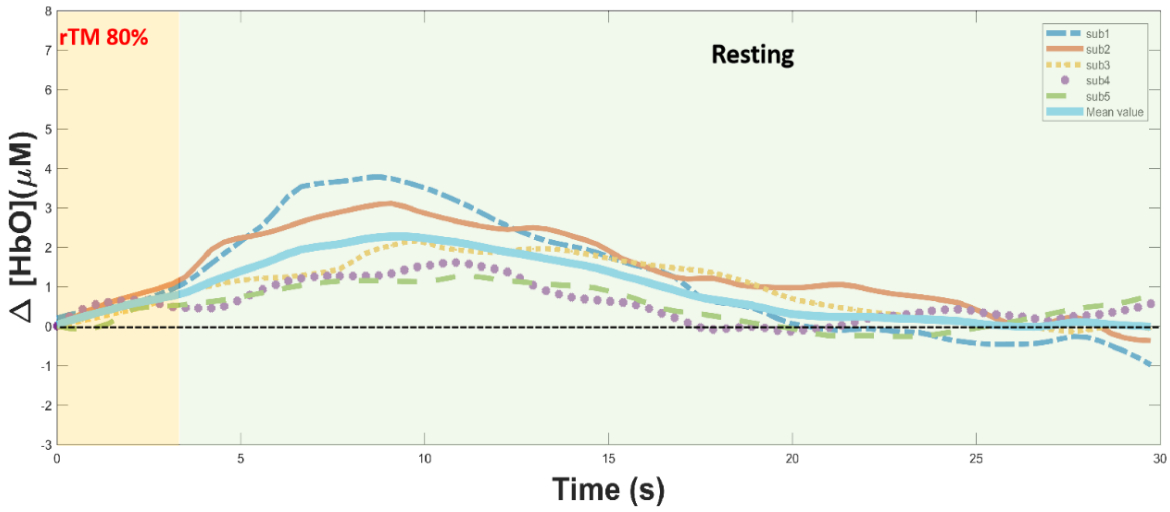

Figure 5.6. Healthy subjects' HbO hemodynamic response during 80% MT TMS stimulation. Time course of averaged oxy-hemoglobin (HbO) for all the subjects under 80% rMT stimulation in the prefrontal cortex. Ten hertz stimulation was performed for 4 s followed by 26 s of rest for 24 epochs. The x-axis represents the time from 0 to 30 s in the epoch, and the y-axis represents the value of HbO concentration in μM/L.

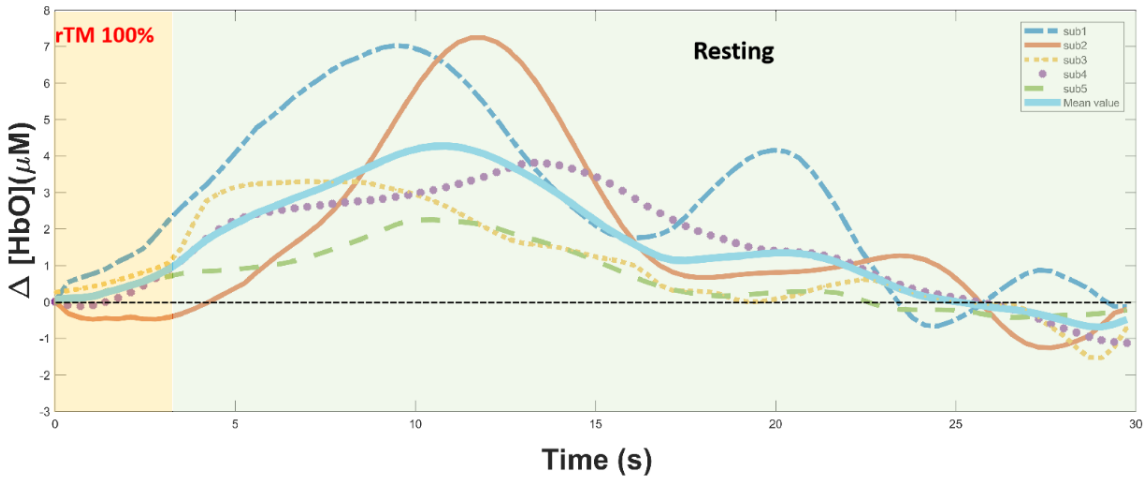

Figure 5.7. Healthy subjects' HbO hemodynamic response during 100% MT TMS stimulation. Time course of averaged oxy-hemoglobin (HbO) for all the subjects under 100% rMT stimulation in the prefrontal cortex. Ten hertz stimulation was performed for 4 s followed by 26 s of rest for 24 epochs. The x-axis represents the time from 0 to 30 s in the epoch, and the y-axis represents the value of HbO concentration in μM/L.

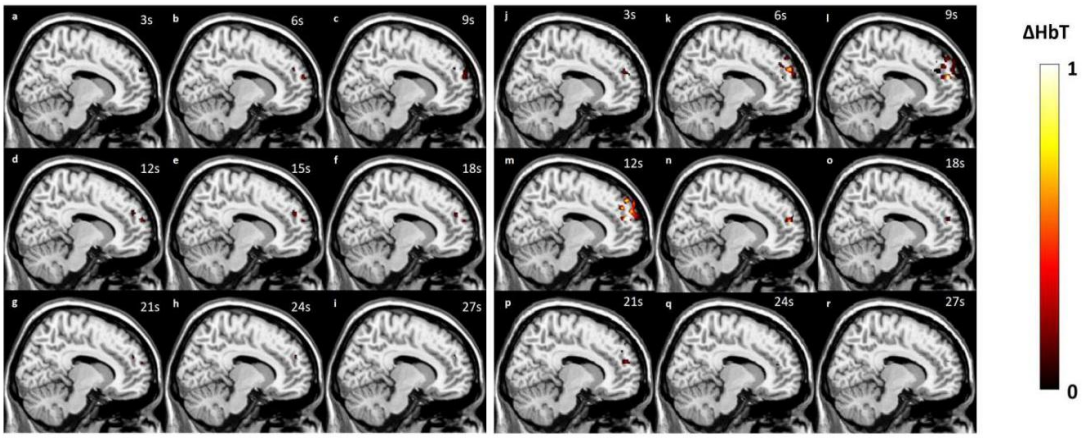

Figure 5.8 Image reconstruction (Sagittal view) for healthy subjects during 80% and 100% MT TMS stimulation. Sagittal section HbT images at selected time points for the 80% (a-i) and 100% (j-r) rMT stimulation.

The average absolute value peak for [HbT] of different rMT stimulation occurs around 10 second and decreased gradually. There was a significant quantitative difference in the [HbT] response between 80% rMT and 100% rMT stimulation. In general, 100% rTM stimulation

response is higher than 80% rTM for each subject and healthy subject 1, 2 are more sensitive than subject 4, 5.

Reconstructed [HbT] images superimposed on the brain MRI in transverse and sagittal sections are shown in Figure 5.8 and 5.9, respectively, using an open source and cross-platform image viewer called MRIcron (https://www.nitrc.org/projects/mricron) where affine transform was applied to register the reconstructed [HbT] space domain to the MRI domain in the MRIcron. We immediately note that the patterns of hemodynamic changes are clearly visualized in the prefrontal cortex region of the brain for both the 80% and 100% rMT for subject 1. We note that the images for 80% rMT stimulation had a more restricted HbT distribution than that for 100% rMT stimulation. Figures 5.8 and 5.9 represent the three-dimensional hemodynamic response change with time. The figure 8 shows the sagittal section that gives the depth information of HbT change with time. And the "8-shape" in Figure 5.9 represents the top view location of the TMS coil on the transverse plane. We notice that the reconstructed images at time point 9s and 12s show more stronger HbT response than other time points. Besides, the reconstructed images represent the HbT response change with time which have consistent tendency results in figure 5.2 and 5.3, which was reliably caputred by our system. These reconstructed images clearly show the volumetric location of hemodynamic response in the brain in different views, which is useful for studying the mechanism of TMS and the pathophysiology of the disorders in which it is applied. In summary, our findings from this pilot experiment are consistent with previous studies with fMRI, fNIRS and optical imaging, where brain activations were found at similar cortex locations.

We immediately note that the patterns of hemodynamic changes are clearly visualized in the prefrontal cortex region of the brain for both the 80% and 100% rMT for healthy subject 1. In these provided figures, clear different pattern has been observed and the 80% rMT stimulation has

a more restricted distribution than 100% rMT stimulation. Affine transform was applied to register the reconstructed [HbT] space domain to the MRI domain in the MRIcron. Our findings are consistent with previous studies with fMRI, fNIRS and optical imaging, where brain activations were found at similar cortex locations.

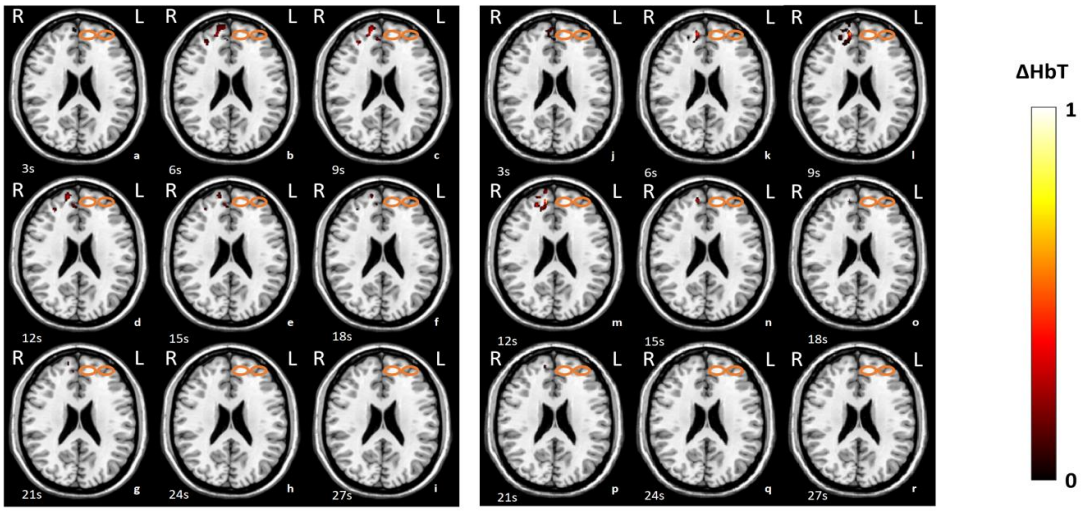

Figure 5.9 Image reconstruction (Transverse view) for healthy subjects during 80% and 100% MT TMS stimulation. Transverse section HbT images at selected time points for the 80% (a-i) and 100% (j-r) rMT stimulation.

5.1.6 Discussion and Conclusion

For the first time to our knowledge, three-dimensional hemodynamic changes in the brain during rTMS have been successfully imaged with diffuse optical tomography. Our results in healthy subjects show a robust increase in [HbT] or activation in the contralateral dorsolateral prefrontal cortex (DLPFC) when comparing 100% intensity vs. 80%. This was coupled with real time image acquisition of the selected areas that displayed these changes visually as well. Such findings create a promising and novel approach of investigating functional connectivity within the

brain and the mechanisms of action that allow rTMS to exert its effects upon various neuropsychiatric disorders.

Previous studies which implemented fNIRS during rTMS with parameters near our experiment's reported the different frequencies and MT stimulation subject to different inhibitory and excitatory results in the brain. Lower frequencies (1 Hz) seem to cause [HbT] decrease in the motor center and prefrontal cortex which has provided a good effect on the treatment for depression while high frequencies (10 Hz) shows [HbT] increasing. Our results presented a similar hemoglobin changes captured in the bilateral cortices, lending support for the reliability of our device [19]. However, in comparison, their spatial resolution and lack of visualization of what areas of the brain were truly being stimulated limited their implication.

Based on our results, DOT is the only modality now that has demonstrated the capability of imaging the brain during rTMS three-dimensionally without significant noise interference. Parameter testing that has already been conducted with fNIRS and other imaging techniques can now be done with DOT. With the additional benefits of volumetric analyses and three-dimensional images, new insights into the neurophysiology of TMS itself can be explored more appropriately. For clinical purposes, the pairing of DOT with TMS may open new paths of discovering how to optimize its treatment of depression and potentially obsessive-compulsive disorder, which was recently approved for treatment by TMS by the Food and Drug Administration in the United States [20]. Very little functional neuroimaging data currently exists for this disorder, despite the potential improvements that could be made to its treatment with TMS [21].

We realize that there were limitations in this study. The number of effective optical data was reduced significantly for some cases due to strong light absorption by hairs. To resolve this issue, we plan to construct improved optical interface that can better contact with the scalp. In

addition, we will attempt to design and develop amplifiers that can improve the signal-to-noise ration. Another limitation was the insufficient number of female participants which prevented us from making any meaningful observation on the difference of brain activation during rTMS in genders. By the way, due to "big interface" limitation, our setup was created to obtain images from the contralateral DLPFC. Directly under the coil and bilateral data collection could have a better understanding about brain activation, however, our results are still the same as previous functional imaging data as fNIRS and fMRI did.

In summary, this is the first work to visualize the rTMS induced brain activation in 3D in humans by DOT. This study suggests that DOT has the potential to provide brain functional parameters during rTMS that may allow for the optimization of rTMS treatment of depression. This study presented the hemoglobin response during different TMS stimulation. We can have a peek into the mechanism of the TMS treatment study in the depression disease. In the future, the DOT imaging system can be utilized for monitoring the hemoglobin response between the depressed patients and healthy subjects.

5.2 Neuroimaging of Depression with Diffuse Optical Tomography During Repetitive Transcranial Magnetic Stimulation [3]

5.2.1 Abstract

Repetitive transcranial magnetic stimulation (rTMS) is a safe treatment method with a good effective ratio for depression; however, the parameters for the treating the depression has likely been hidden and unclear due to non-optimized targeting. Certain important reasons such as unclear

[3] This section 5.2 was published in the Scientific Report that is affiliated with Springer Nature Journal. Jingyu Huang and Shixie Jiang are co-first author with equal contribution. Jingyu Huang did the experiment and generated the figures and results including wrote the initial manuscript. Shixie Jiang corrected the English and extend the analysis of final results in clinical method. Shixie Jiang also wrote the protocol and IRB for the depression study. Hao Yang, Ryan Wagoner, F Andrew Kozel, Gleen Currier are assistance and doctors to recruit the subjects in the clinical study. Huabei Jiang is the telecommunication author. Permission is included in Appendix B.

ideal stimulation parameters, lack of information regarding can stop the study about how the brain is physiologically reacted during and after the repetitive transcranial magnetic stimulation. While neuroimaging is ideal for obtaining such critical information, existing modalities have been limited due to poor resolutions, along with significant noise interference from the electromagnetic spectrum. In this study, we utilized diffuse optical tomography (DOT) device, a novel and non-invasive technology, in order to improve our understanding for the neurophysiological effects of rTMS in depression.

In this study, healthy and depressed subjects from the age of 18 to 70 were recruited. All the treatment parameters were followed by FDA depression treatment with targeting the left dorsolateral prefrontal cortex under a 100% magnetic field intensity of motor threshold. TMS pulse frequency is 10 per second with a 4 second stimulation time and a 26 second rest time for each trial. DOT imaging system was simultaneously capturing the brain activation from the contralateral dorsolateral prefrontal cortex.

For the results, the final analysis consists of the results of six healthy and seven depressed subjects. Hemoglobin response and volumetric three-dimensional activation patterns were successfully captured. When comparing the results with the healthy subject group, depressed subjects were found to exist a delayed and less robust response to rTMS.

In this first-in-human study, the results published in the paper proves the ability of DOT, which demonstrates this technology can safely and reliably reach and capture cortical response patterns to rTMS in depressed and healthy subjects. In the next section, we would gradually introduce this non-invasive optical functional imaging modality to investigate the brain targeting, and how to reach the more effective new treatment parameters in depression treatment. The results would prove this is a novel approach in the neuropsychiatric disorder treatment.

5.2.2 Introduction

Major depressive disorder is a chronic, recurrent, and debilitating mental health illness linked to significant functional impairment, disability, and mortality [22]. It is the primary cause of mental health-related disease burden globally, affecting approximately 300 million individuals [23]. Although there have been numerous clinical trials and studies on existing pharmacological and non-pharmacological options, its overall treatment is still challenging [24]. The largest and most extensive trial, the Sequenced Treatment Alternatives to Relieve Depression (STAR*D), revealed that antidepressants, even with augmentation, demonstrated suboptimal remission rates [25]. In lieu of medications then, a concerted effort has been dedicated to studying other treatment options, such as brain stimulation techniques. Transcranial magnetic stimulation (TMS) has now been established over the past decades as a safe and effective treatment for depression [26].

Repetitive transcranial magnetic stimulation (TMS) was cleared by the Food and Drug Administration (FDA) for the treatment of depression in 2008 [27]. When TMS is administered repeatedly at a specific frequency, it is referred to as rTMS. It involves passing an electrical current through an insulated coil, which creates an alternating magnetic field that penetrates the scalp and skull to induce neuronal depolarization and modulation [28]. Several landmark trials were conducted that reliably demonstrated its efficacy and safety in improving depressive symptoms [29-32]. However, despite its increasing use, the typical effect sizes have been modest at best. A previous meta-analysis of 29 studies and 1371 patients reported only a 29% average response rate and 19% average remission rate in randomized trials [33]. The effectiveness of TMS is likely reduced due to: (1) non-optimized targeting, (2) unclear ideal stimulation parameters (e.g., patterns, frequencies, dosage), and (3) a lack of understanding of how the brain is physiologically responding, during and after, stimulation [34]. In this situation, neuroimaging with rTMS

stimulation would become a particularly promising area because of those questions can probably answered depends on the neuroimaging research results.

Theoretically, the ability for the brain imaging technology have been approved considering of offering valuable information in order to solve the above unanswered questions during the stimulation of TMS. However, due to the immediate brain response would happen occasionally, few modalities can be utilized to possess the temporal resolution required to appropriately evaluate such conditions. Previous studies for analysis the brain activation and connectivity during TMS stimulation include the usage of functional magnetic resonance imaging (fMRI), magnetoencephalography (MEG), electroencephalography (EEG), and functional near-infrared spectroscopy (fNIRS) [35-38]. As fMRI, MEG, and EEG use signals that involve the electromagnetic spectrum, their overall resolution and quality are subject to significant measurement artifacts given the fact that TMS produces very strong magnetic and electrical fields. Due to this, fNIRS has been investigated for concurrent imaging as it measures an optical signal, which has no electromagnetic interference. A portable, safe, cost-effective, and with less restriction can benefits the TMS study considering with other unportable and complicated devices. However, fNIRS has several technical limitations including scalp interference, shallow imaging depth, low spatial resolution, and an inability to produce three-dimensional images [39].

Diffuse optical tomography (DOT) is a noninvasive imaging technology based on the scattering and absorption properties of non-ionizing near-infrared light in biological tissue. It can be treated as an extension and improvement to fNIRS. Diffuse optical tomography is using multiple near-infrared wavelengths, it is able to accurately measure the relative deoxygenated ([Hb]), oxygenated ([HbO]), and total hemoglobin ([HbT]) concentrations for the tissue study. As for the method of image reconstruction, the sophisticated image reconstruction algorithms contains

with inverse problem can generate quantitative three-dimensional images of changes in regional blood volume and oxygenation at high temporal and spatial resolutions [40. This allows DOT to distinguish between hemodynamic response with time [41]. Over the past decades, it has been successfully used clinically for imaging of epilepsy, breast cancer, osteoarthritis, and cortical activations [42-45]. Impressively, it has been demonstrated that DOT is able to detect hemodynamic responses equivalent to fMRI in terms of spatial resolution (within a depth of 5 cm) [46]. With the similar theory to fNIRS, DOT also presents the advantages of being portable, safe, and cost-effective.

The basic aim and objective of this study were to demonstrate DOT technology is a safe, effective, and feasible option for noninvasive, connectivity based functional imaging of the brain during and after rTMS utilized for the healthy and depressed people. We hypothesized that rTMS would produce cortical activation patterns that would be reliably captured by DOT. In addition, we proposed that the with the hemodynamic changes, especially in terms of volume, between healthy and depressed individuals would offer new knowledge and have an opportunity to peak into how neuroimaging can be further used to improve TMS parameters and our understanding of the physiologic effects of brain stimulation [70].

5.2.3 Methods and Materials

5.2.3.1 Study Sample

Recruited subjects were including individuals with no previous or current history of a psychiatric disorder (healthy control group) and those with a current Diagnostic and Statistical Manual of Mental Disorders, 5th Edition (DSM-5) diagnosis of major depressive disorder (depressed group) from the age of 18 to 70. Exclusionary criteria for study participation included a previous history of psychosis, bipolar disorder, posttraumatic stress disorder, eating disorder, or

obsessive-compulsive disorder; pregnancy; personal or immediate family history of a seizure disorder; presence of ferromagnetic material in the head, neurologic disorder, or medication capable of altering the seizure threshold; vague nerve stimulation implant; or history of electroconvulsive therapy failure [71].

The research protocol was approved by the University of South Florida Institutional Review Board. All the methods with the involving human subjects, were conducted in accordance to standard protocols mandated by the Institutional Review Board [71]. The information of the written consent was appropriately obtained by each subject (depressed and healthy) prior to enrollment in the study [70]. Additional informed written consent was also completed by one subject for permission to publish their image in any hard-copy, online, and/or open-access journal article (Figure 1b). A physician screened participants with a Structured Clinical Interview for DSM-5 [47], Transcranial Magnetic Stimulation Adult Safety Screening Questionnaire [48], a medical history review, and a physical exam. Routine laboratory studies including a complete blood count, complete metabolic panel, thyroid stimulating hormone, urine toxicology screen, urine pregnancy test (if the participant was a woman of child-bearing potential), and electrocardiogram were obtained during the screening process. Subjects were required to be medically stable before enrollment [71].

5.2.3.2 rTMS Procedure

All rTMS treatments were performed with a Neurostar TMS Therapy System (Neuronetics, Inc., Malvern, PA, USA). Stimulation protocol was followed per the product documentation. Subjects were placed in a recliner and ear plugs were inserted to minimize possible hearing impairment from the TMS machine noise. The location of the motor strip was estimated by stimulating the cortex at low frequency (1 Hz) and device output (45%), advancing the power and

repositioning the coil to elicit a reliable (5 out of 10 trials) muscle twitch of the abductor pollicis brevis in the appropriate contralateral hand [49]. Using the TMS Motor Threshold Assessment Tool, the motor threshold (MT) was determined four times and averaged [50]. Treatment parameters were standardized for each individual at the left dorsolateral prefrontal cortex (DLPFC) (Neurostar standards) with a 100% magnetic field intensity of MT, with a pulse frequency of 10 per second which consists of a 4 second stimulation time and a 26 second stimulation rest time. In total, the interval time and stimulation time have a total 3000 delivered pulses per experiment.

5.2.3.3 DOT Procedure

All imaging was captured by a custom built fast multispectral DOT imaging system constructed from our laboratory's previous studies [51]. The system involves a main computer sending a signal to a light emitting diode (LED) controller which activates two groups of LEDs (48 optodes per group; one group at 780nm and the other at 850nm) (High-power NIR LEDs, Epitex, Inc.). Two core boards (CuteDigi Technologies), consisting of an Altera EP2C8 FPGA, 50-megahertz crystal oscillator, and 139 input/output pins, were used to control the time sequences of each LED [71]. The light beams were sequentially delivered to the measuring interface through fiber optical bundles. The subsequent diffusing light from the tissue was received by 48 highly sensitive avalanche photodiode detectors (APD C5460-01, 12-bit resolution, maximum analog-digital conversion rate of 1.25 mega-samples/second) and converted to electrical signals for further processing. Continuous-wave measurements of three-dimensional data were captured through the 48 pairs of highly sensitive photo source-detectors. A full set of high density tomographic optical data was acquired with a unit consisting of two PCI-DAS6071 boards at a 14.4 Hz collection rate for both the wavelengths [70].

Participants were positioned in the TMS device chair and adjusted to ensure comfort throughout the experimental procedure. We utilized a two-layer interface coupled with a 256-channel medium-sized EEG cap capable of fitting the head size of all of our subjects (Figure 1). All external light was blocked from entering the clinical lab, and the ambient lighting was tested to ensure that it did not contaminate the DOT signal. The DOT probe, consisting of the 48 pairs of source-detectors, was then positioned over the right prefrontal cortex. The probe was fastened using Velcro straps and attached against the scalp with the tips directly touching the skin for maximum efficiency of light transmission. Any hair strands under the probes were manually moved away using combs to facilitate optimal contact and avoid contamination by light absorption. The subjects were then instructed to sit quietly, remain awake, not move, and keep their eyes open. DOT data acquisition occurred 1 minute prior to stimulation, during the 24 stimulation/rest epochs (30 s per epoch), and during a 2-minute post stimulation period, resulting in a total recording time of 15 minutes.

In this study, the depressed patient can only capture one side of the brain activation. In the future, with the development of the neuro-imaging modality in the future, although the theory and the reason for the treatment of TMS is unclear, the researchers can establish a connectivity analysis method to analyze the different region of brain to advance the TMS treatment in the clinical study.

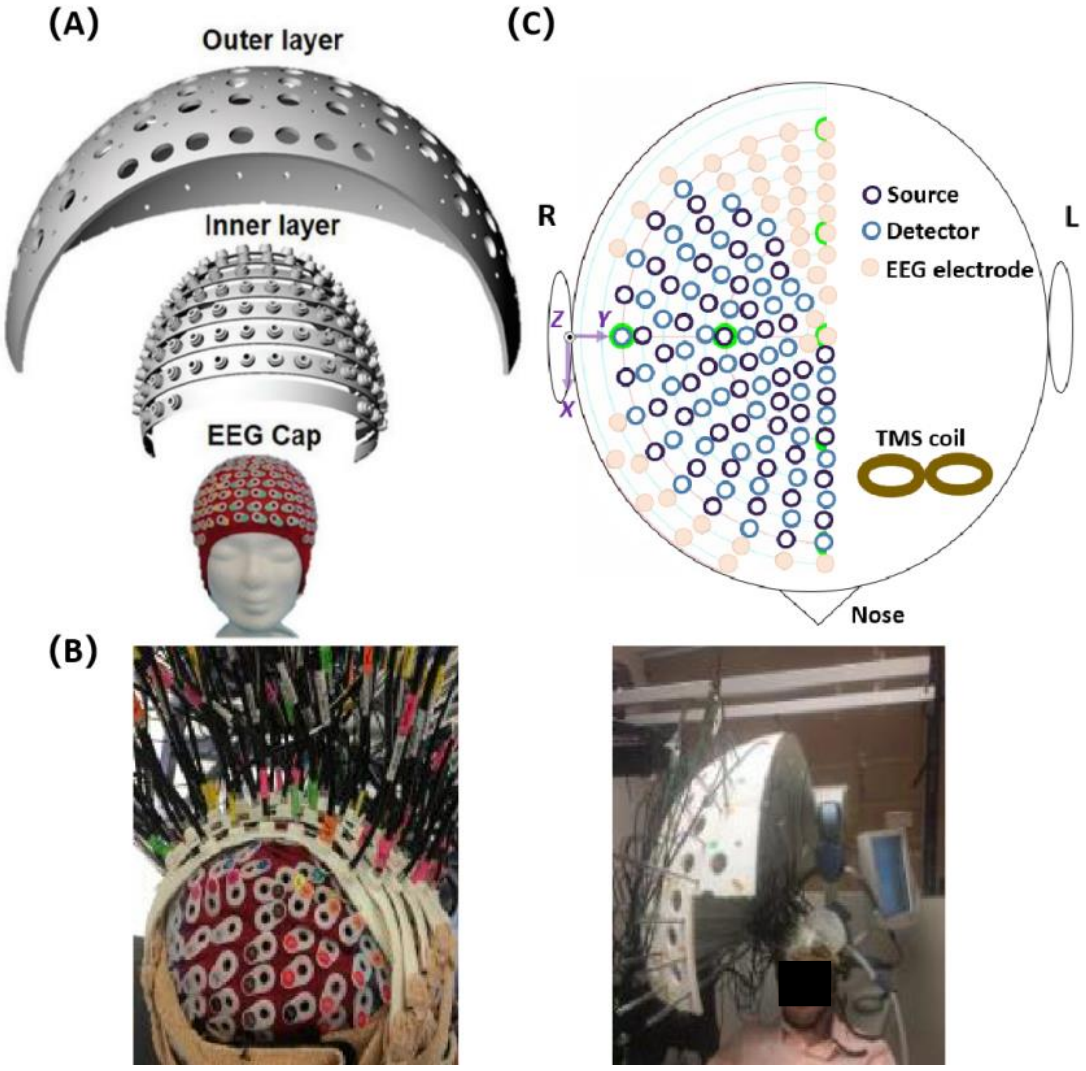

Figure 5.10 Custom DOT brain interface. A) Two-layer design with an inner and outer layer superimposed upon a modified electroencephalogram cap; B) Photographs of the interface connected to a human subject; C) Top-down schematic depicting the location of the TMS coil (light brown figure of eight symbol) over the left dorsolateral prefrontal cortex and the DOT cap over the contralateral side. The probe comprised of 48 source-detector pairs in total.

5.2.3.4 Image Analysis and Processing

The DOT data were processed and analyzed channel-wise (one channel represents one source-detector pair). The setup comprised of 48 channels in total. The raw data for each channel

were inspected during the entire experiment time course in order to exclude epochs with significant discontinuity. Several channels had epochs with inadequate measurements due to suspected motion artifact, thus were removed accordingly. After ensuring the quality of the data, we used a band pass filter (cut off frequencies f_H =9 Hz, f_L =0.02 Hz) to exclude instrumental noise and saturated signals. Contamination of signal from peripheral co-stimulation during TMS is inherently prevented by the DOT reconstruction algorithms which include boundary limits when calculating the data from the high number of source-detector pairs. Data were averaged for all participants and the resting time in the experiment was used as the baseline. The high-density tomographic data acquired at each wavelength was used to reconstruct a three-dimensional image of tissue absorption coefficient using a finite element-based algorithm previously developed and optimized [52]. The physiological measurements in terms of oxygenated and deoxygenated hemoglobin, [HbO] and [Hb], respectively, were calculated using the absorption coefficient images at both wavelengths and a modified Beer-Lambert law coupled with a least-square fitting procedure through pseudo-inverse matrix calculations [53]. Cerebral blood volume was estimated by calculating the total hemoglobin concentration, [HbT], which was achieved by summing [HbO] and [Hb].

5.2.3.5 Definition of Regions of Interest

The coordinate system used was based on a Cartesian three-dimensional configuration combined with a 256 channel EEG system. The origin [0, 0, 0] was set at C18 on the EEG system. The EEG cap has covered the full prefrontal cortex which is our main region of interest for the depression study. The TMS coil was located at left DLPFC while our DOT interface cover at the right DLFPC. The interest of area is the DLPFC in the TMS study. From this location, three-dimensional images including coronal, sagittal, and transverse views were derived. The direction

of the X, Y, and Z axes were defined as right to left, posterior to anterior, and inferior to superior. The right prefrontal cortex was centered at coordinates [51, 35, 53] for the healthy subjects. For the depressed group, this location was centered at coordinates [48, 39, 57].

5.2.3.6 DOT Statistical Analysis

Data analysis was conducted using MATLAB (version R 2018a) and SAS (9.4). Subject means were allowed to vary around an individualized intercept across trials with stimulation type as a within subject factor. Redundant analysis was conducted using repeated measures analysis of variance (ANOVA) to allow simpler interpretation of the results. The alpha level was set at 0.05 for all calculations.

5.2.4 Results

5.2.4.1 Participants

Eight healthy individuals (7 men and 1 woman) with a mean age of 33.5 ± 15.9 years and eleven depressed patients (2 men and 9 women) with a mean age of 51.8 ± 15.7 years were initially recruited as paid volunteers. Two healthy subjects were excluded due to significant motion artifacts that could not be rectified. Four depressed subjects were excluded due to weak signal processing and volitionally leaving the experiment prior to completion of data collection. In total, six healthy individuals (5 men and 1 woman) with a mean age of 36.3 ± 16.7 years and seven depressed individuals (2 men and 5 women) with a mean age of 49.1 ± 17.8 years were included for final analysis. All the participants were right-handed, as determined by the modified Edinburgh Handedness Questionnaire [54], and had normal or corrected-to-normal vision. All subjects were of Caucasian descent except for two Asian females (one from each study group). For the depressed individuals, all of them had failed at least 3 antidepressants, been diagnosed by a psychiatrist for

at least 3 years with Major Depressive Disorder, and remained on antidepressants while receiving rTMS treatment.

5.2.4.2 DOT Imaging Data

As hypothesized, there was an observable quantitative difference in the hemodynamic response between healthy and depressed subjects within the right dorsolateral prefrontal cortex. In healthy individuals, [HbO] and [HbT] began to increase sharply beginning at 2.62 seconds until a peak observed at 10.40 seconds (95% CI [1.544, 9.609] and [1.734, 6.220] for [HbO] and [HbT], respectively). The average absolute value of hemoglobin change was calculated to be 5.58 μM and 3.98 μM for [HbO] and [HbT], respectively. [Hb] was found to decrease in a reciprocal manner at first until 5.3 seconds, with a gradual decline thereafter for the rest of the epoch. Its average absolute value was calculated at 3.04 μM (Figure 2). In the depressed subjects, [HbO] and [HbT] increased more gradually and their values plateaued later in comparison to the healthy subjects at 14.55 seconds (95% CI [1.869, 4.169] and [1.108, 2.462] for [HbO] and [HbT], respectively) ($p=0.013$ for [HbO] and $p=0.011$ for [HbT]). The average absolute values of hemoglobin change in this group were noted to be decreased, at 3.98 μM and 2.27 μM for [HbO] and [HbT], respectively. [Hb], in a similar fashion, decreased gradually though reached a nadir later at 18.43 seconds (Figure 3). The average value of change was calculated to be 2.71 μM.

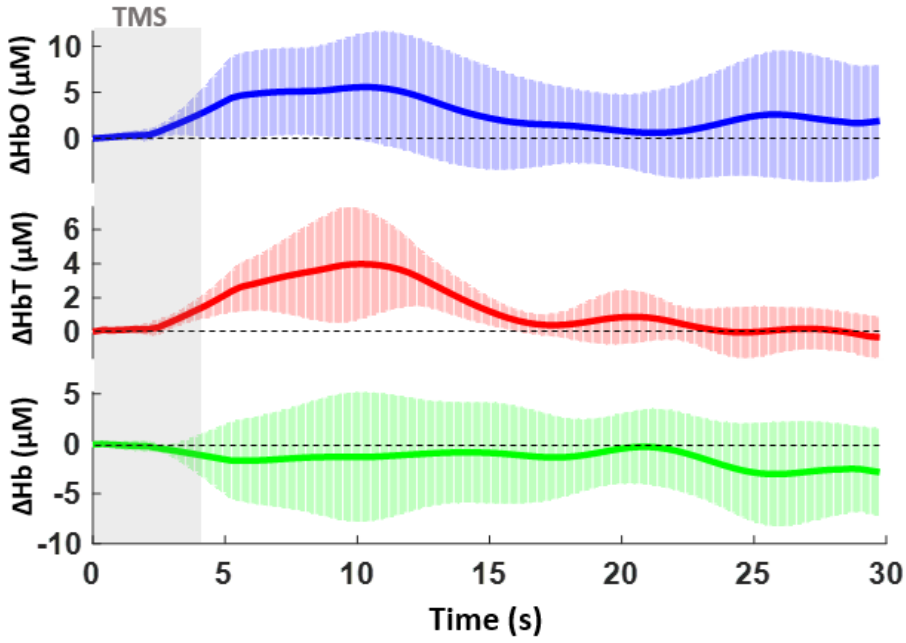

Figure 5.11 Hemoglobin response for healthy subjects during TMS treatment stimulation. Averaged time course of oxygenated [HbO], total [HbT], and deoxygenated [Hb] hemoglobin signals in the healthy subjects for the contralateral or right dorsolateral prefrontal cortex. Ten hertz stimulation was performed for 4 s followed by 26 s of rest for a total of 12 epochs.

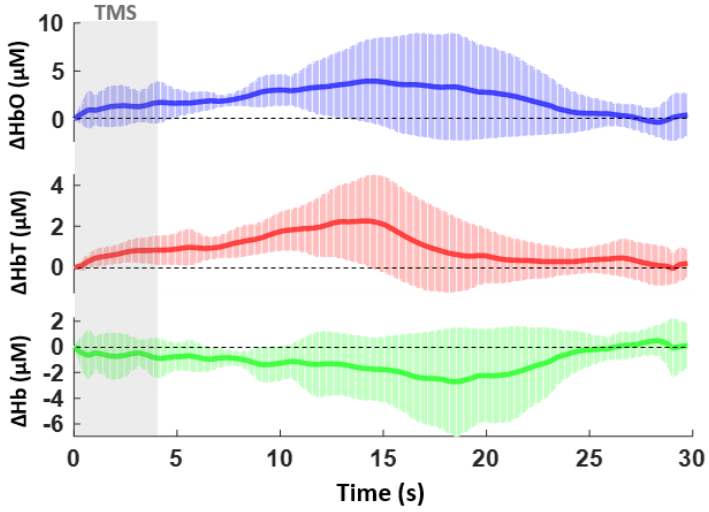

Figure 5.12 Hemoglobin response for depression patients during TMS treatment stimulation. Averaged time course of oxygenated [HbO], total [HbT], and deoxygenated [Hb] hemoglobin signals in the depressed subjects for the contralateral or right dorsolateral prefrontal cortex. Ten hertz stimulation was performed for 4 s followed by 26 s of rest for a total of 12 epochs. The x-axis represents the time from 0 to 30 s during the epoch and the y-axis represents the mean and standard deviation for relative hemoglobin concentration in μM/L.

When comparing the two groups, the difference in time to peak [HbO] and [HbT] was 4.15 seconds ($p=0.032$ for [HbO] and $p=0.010$ for [HbT]), with a later onset in the depressed subjects. The average hemoglobin change in this group was also observed to be decreased by 1.60 μM, 1.71 μM, and 0.33 μM for [HbO], [HbT], and [Hb], respectively.

Three-dimensional functional imaging during and after rTMS stimulation was successfully captured by our DOT system. In the provided transverse and sagittal images of the right DLFPC (Figures 5.9 and 5.10), clear distinctions in activation patterns between a depressed and healthy subject can be observed. Healthy subjects were observed to have a more robust area of activation prior to a return to baseline. In comparison, depressed individuals had a smaller change in hemodynamic response with a more restricted distribution pattern. By taking advantage of the inherent ability of DOT to assess depth, a volumetric analysis of the change in [HbO] was also calculated. During the 4 seconds of stimulation, alterations in the volume (in cm^3) of activation were observed to occur, which continued even after cessation of stimulation. Healthy subjects reached a maximum average volume change of 6.99 cm^3 whereas depressed subjects peaked at 2.95 cm^3 ($p=0.016$). As can be seen in Figure 6, we were able to concurrently plot volume changes with three dimensional images in our subjects. An increase in volume stimulated can clearly be seen in both groups that peaks and then gradually trends towards baseline, with a smaller volume of response in the depressed group.

For these results, we got the hemodynamic response for both healthy and depressed patient groups under the same TMS stimulation. We captured the volume of brain activation for both groups, that can have a clear comparison of the sensitivity for different groups. The hemodynamic response change with time and the image reconstruction can validate the results about the brain activation for both groups. Three-dimensional DOT image reconstruction can give us the depth

information for brain activity, that can help the doctor monitor the treatment of depression. The prefrontal cortex stimulation for TMS was treated as the golden treatment for the depressed patients who do not have good reaction about the medication treatment. In this case, our DOT imaging system can offer a good evaluation system to help doctor treat the depressed patients.

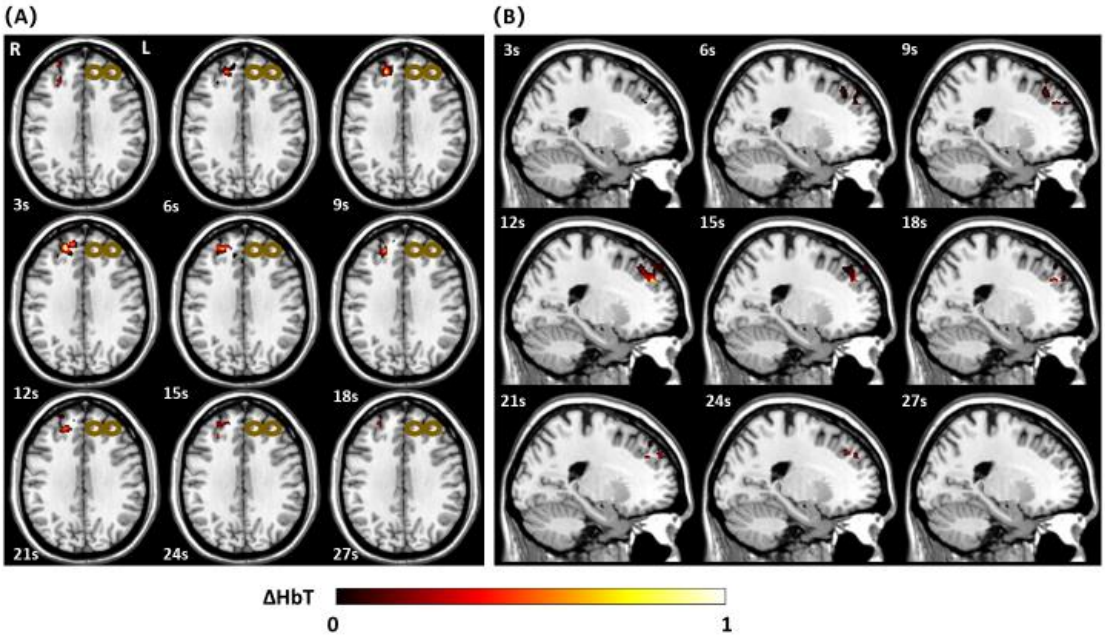

Figure 5.13 Healthy subjects image reconstruction during TMS treatment stimulation. A) Transverse view of the three-dimensional [HbT] images collected by DOT in a healthy subject during a 30 s epoch. B) Sagittal view of the three-dimensional [HbT] images collected by DOT in a healthy subject during a 30 s epoch. Data was only acquired from the right hemisphere of the brain. The bronze colored coil symbol represents stimulation of the left side.

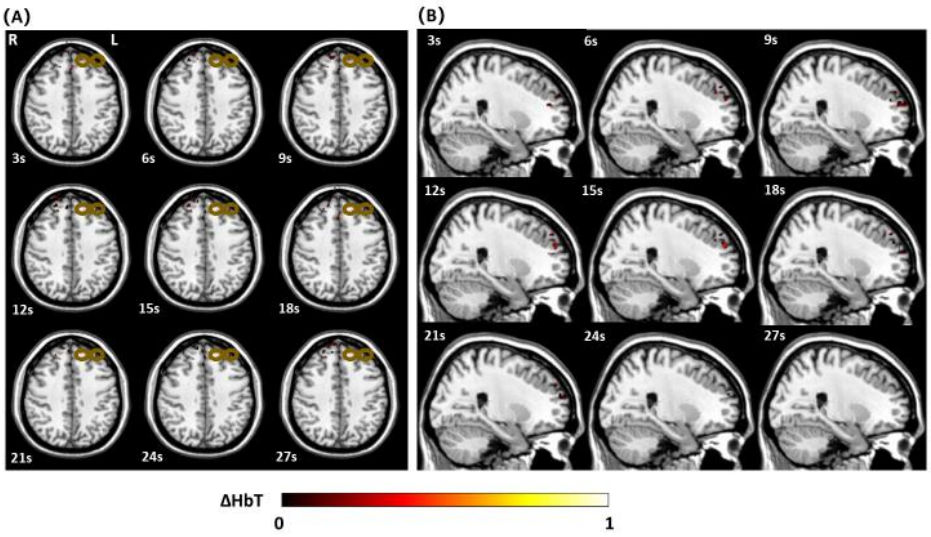

Figure 5.14 Image reconstruction for depression patients during TMS treatment stimulation. A) Transverse view of the three-dimensional [HbT] images collected by DOT in a depressed subject during a 30 s epoch. B) Sagittal view of the three-dimensional [HbT] images collected by DOT in a depressed subject during a 30 s epoch. Data was only acquired from the right hemisphere of the brain. The bronze-colored coil symbol represents stimulation of the left side.

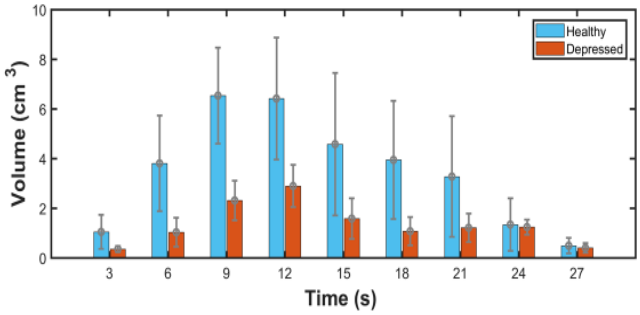

Figure 5.15 Averaged volume changes between healthy and depressed groups. Averaged volume change (in cm^3) with error bars of [HbO] signal compared between the healthy and depressed groups.

5.2.5 Discussion

In this study, we have demonstrated for the first time the ability of a novel DOT system to capture cerebral hemodynamic activity during and after rTMS in depressed and healthy

individuals. Previous studies with fNIRS and other modalities have only been able to offer incomplete insights due to the lack of adequate temporal and spatial resolution, and more importantly, volumetric three-dimensional images. Many of those experiments focused on lower frequency stimulation in healthy subjects as well. No prior study has directly compared depressed individuals with healthy ones, especially using treatment parameters closer to those that are approved by the FDA in the United States. As such, the implications of our findings potentially create a new frontier in furthering our knowledge of the mechanism of TMS in depression and how we can improve it to more effectively treat depression.

A plethora of past fNIRS studies have observed how different frequencies and motor thresholds of TMS stimulation cause variable inhibitory or excitatory effects within the brain. Lower frequencies (1, 2, 5 Hz) tend to cause decreases in [HbO] in the motor or prefrontal cortices, and previous studies have demonstrated that 1 Hz stimulation on the right DLPFC has a clinical effect on treating depression. 10 Hz stimulation has been shown to increase [HbO], which was associated with continued therapeutic effects of TMS [55-57]. Our results show a clear difference in the time to peak [HbO] and [HbT] and average hemoglobin value change between depressed and healthy subjects. There is a noticeable delayed and decreased hemodynamic change that likely reflects a less robust response to rTMS treatment. The reasoning underlying this finding is possibly linked to what is occurring at the neuronal or cellular level. The neurobiology and pathophysiology of depression is a much-debated topic without any definitive conclusions. There is suspected to be a complex interplay within multiple realms including neurocircuitry, molecular signaling, genetics and epigenetics, homeostatic adaptations, and immune responses [58]. An exact circuit has not been identified, though several regions have been noted to be malfunctioning including the orbitomedial prefrontal cortex, anterior cingulate cortex, amygdala, hippocampus, cerebellum, and

basal ganglia [59]. Within these areas, one such hypothesis suggests that there are redundant and dysfunctional firing of neurons which leads to overall decreased activity, and thus reduced neurovascular coupling and blood flow, which is potentially what is being observed in our depressed subjects [60].

In terms of our volumetric three-dimensional analyses, we also observed distinct differences in the time to maximum volume change between depressed and healthy subjects. At 12 seconds (or 8 seconds after the stimulation window), depressed subjects only reached approximately half the depth of hemodynamic change that healthy individuals experienced. Although DOT is unable to reliably obtain data of the deepest structures within the brain, this finding may further reinforce the rationale underlying theories about what TMS is truly stimulating in depression. The left DLPFC is the most common target for treating depression not only necessarily due to this specific region itself, but from studies demonstrating that it modulates the blood flow response and activity of the anterior cingulate cortex as well [61]. The rates of perfusion and metabolism in this region in particular may predict response to treatments [62]. Thus, our depth analyses may demonstrate that either our treatment parameters were not adequate enough to generate appropriate activation or again, that depressed individuals at baseline have reduced hemodynamic responses.

The significance of our data then may potentially pave the way towards truly optimizing TMS for depression at even the individual level. Ideal stimulation parameters have remained unknown as there has previously been no reliable mechanism to measure neural connectivity and responses in real time. Utilizing DOT simultaneously with TMS in testing variable frequencies, intensities, number of pulses, and interval timings offers a new promising approach to allowing such exploration in real time and with three dimensional images. Cortical activation/inhibition

patterns and hemodynamic responses would be reliably captured in depressed and healthy individuals. In addition, pairing DOT with newer protocols such as intermittent theta burst stimulation (iTBS) may also lend further credence to such approaches. iTBS uses 50 Hz triplet "bursts" every 200 ms to activate the brain and deliver an entire therapeutic dose equivalent of stimulation in 3 to 10 minutes versus the standard 18 to 37 minutes. Recently Cole et. al published the first trial demonstrating a high efficacy when delivering iTBS ten times daily for five days, thus dramatically shortening the usual treatment time [63]. To the best of our knowledge, no neuroimaging studies have been conducted which compare iTBS or other techniques with traditional 10 Hz rTMS, which a direct comparison may offer even further insights into discovering optimal parameters. Additionally, using a modality like DOT to study iTBS by itself may help us understand this particular technique more as well.

Another unanswered question of how TMS can be improved involves developing more precise stimulation site targeting. Traditionally, providers will identify the left DLPFC by the "5-cm rule," which involves finding the area over the motor cortex that produces a finger twitch, then moving 5-6 cm anterior [64,65]. As there are inherent differences in neuroanatomy, this method may lead to enormous treatment response heterogeneity among individuals [66]. It has been recently speculated that structural magnetic resonance imaging-guided placement of the coil may lead to improved outcomes; however, this has not been established [67]. Instead, targeting with fMRI has preliminarily shown improved antidepressant response if stimulated at more anterior and lateral locations within the DLFPC or at a site more negatively correlated to the subgenual cingulate [68,69]. Unfortunately, it is very challenging to reliably use fMRI simultaneously with TMS. Additionally, these machines are quite expensive, not portable, and not readily available in many areas of the world. DOT on the other hand would be able to theoretically assist with targeting

in a similar fashion as the area that requires identification is superficial enough to be within standard DOT imaging depths.

Our study was certainly not without limitations. First, this was a pilot study with a heterogeneous, small sample size at a single center, without randomization or a TMS sham group. As such, the generalizability of our results is limited due to the inherent design. Additionally, due to the small sample size, age and gender-related cortical atrophy may affect results given the coil to cortex distance theoretically; though the average age of our groups was not within the range at which atrophy rates increase significantly. We also did not conduct any regular standardized symptom scales or assessments throughout that would allow us to comment on TMS treatment efficacy differences within the depressed group. Next, the intensity of our TMS parameters was set at 100% instead of 120% which could certainly affect the neural activation patterns captured by imaging. Our parameters otherwise were within FDA approved limits for the treatment of depression. For initial feasibility purposes, the DOT setup was created to obtain images from the contralateral DLPFC. Directly under the coil and bilateral data acquisition would have been more ideal, as fNIRS can be used in such a way. However, our results were still congruent with previous functional imaging data and future directions include augmentation of the setup to obtain bilateral information in subsequent studies.

In addition, further obstacles regarding the DOT setup itself should be mentioned. Due to the physical limitations of the optical fibers and optodes used in the headgear design, meticulous planning of the array must be considered. Movement artifacts, as with any other techniques, is still a significant barrier that will inevitably be present. Proper construction of the optode headgear with fixation may assist with reducing this phenomenon, along with further advancements in post-processing and filtering methodologies. Physiological signal contamination is another technical

limitation that is common to all optical methods especially. Although DOT suffers much less from scalp interference (compared to fNIRS), the presence of hair itself or dark shades impairs signal quality. As such, pinning or separation of hair is an unideal and imprecise method often employed. Further development of analysis and filtering algorithms may assist with bypassing this issue. Lastly, the maximum depth that can be reliably and accurately imaged is greater than fNIRS, though is still limited compared to fMRI. It is estimated to be approximately 5 cm, which reduces the ability to detect deeper brain structures, but more than capable of capturing cortical and some subcortical structures.

5.2.6 Conclusion

In summary, this is the first study to our knowledge of using DOT to simultaneously measure functional brain changes induced by rTMS in depressed and healthy subjects. Standard treatment parameters were conducted along with concurrent neuroimaging that demonstrated a delayed and less robust response in depressed individuals. Real time, three-dimensional images with high spatial and resolution were collected, along with associated volumetric changes. This novel optical neuroimaging device is a safe, noninvasive, portable, and effective modality that may pave the path towards furthering our understanding of neural connectivity in depression and with further studies may allow for optimization of treatment parameters and thus improved outcomes in depression.

5.2.7 References

1. McConnell K.A, Nahas Z, Shastri A, *et al*. The transcranial magnetic stimulation motor threshold depends on the distance from coil to underlying cortex: A replication in healthy adults comparing two methods of assessing the distance to cortex. *Biological Psychiatry* 49(5) (2001), 454–459.

2. Somani A and Kar S.K. Efficacy of repetitive transcranial magnetic stimulation in treatment-resistant depression: the evidence thus far. *General Psychiatry* 32(4) (2019), e100074.

3. Abraham T and Feng J, Evolution of brain imaging instrumentation. *Seminars in Nuclear Medicine* 41(3) (2011), 202–219.

4. Kozel F.A, Tian F, Dhamne S, *et al*. Using simultaneous repetitive Transcranial Magnetic Stimulation/functional Near Infrared Spectroscopy (rTMS/fNIRS) to measure brain activation and connectivity, *NeuroImage* 47 (2009), 1177.

5. Pridmore S, Fernandes Filho JA, Nahas Z, Liberatos C, George MS. Motor threshold in transcranial magnetic stimulation: a comparison of a neurophysiological method and a visualization of movement method. *J ECT*. 1998 Mar;14(1):25-7.

6. Borckardt J.J, Nahas Z, Koola J and George M.S. Estimating resting motor thresholds in transcranial magnetic stimulation research and practice: a computer simulation evaluation of best methods, *J ECT* 22(3) (2006), 169–175.

7. Horvath J.C, Mathews J, Demitrack M.A and Pascual-Leone A. The NeuroStar TMS device: conducting the FDA approved protocol for treatment of depression. *Journal of Visualized Experiments* 45 (2010), 2345.

8. Yang J, Zhang T, Yang H and Jiang H. Fast multispectral diffuse optical tomography system for in vivo three-dimensional imaging of seizure dynamics. *Appl Optics* 51 (2010), 3461–3469.

9. Smith A.M, Mancini M.C and Nie S. Bioimaging: second window for *in vivo* imaging. *Nature Nanotechnology* 4(11) (2009), 710–711.

10. Jiang H, *Diffuse Optical Tomography: Principles and Applications* (1st ed.), Gainesville, 2010, CRC Press.

11. Dai X, Zhang T, Yang H, *et al*. Fast noninvasive functional diffuse optical tomography for brain imaging. *J Biopho-tonics* 11(3) (2018), 10.1002/jbio.201600267.

12. Custo A, Boas D.A, Tsuzuki D, *et al*. Anatomical atlas-guided diffuse optical tomography of brain activation. *Neuroimage* 49 (2010), 561–567.

13. Zhang T, Zhou J, Carney P.R and Jiang H. Towards real-time detection of seizures in awake rats with GPU-Accelerated diffuse optical tomography. *Journal of Neuroscience Methods* 2015, 240,28-36.

14. Jiang H, Paulsen K.D, Osterberg U.L, *et al*. Optical image reconstruction using frequency domain data: simulations and experiments. *J Opt Soc Am A* 13 (1996), 253–266.

15. Wu C, Barnhill H, Liang X, *et al*. A new probe using hybrid virus-dye nanoparticles for nearinfrared fluorescence tomography. *Opt Commun* 255 (2005), 366–374

16. Jiang H, *et al*. Frequency-domain fluorescent diffusion tomography: a finite-element-based algorithm and simulations, *Appl Opt* 37 (1998), 5337–5343.

17. Bluestone A.Y, Stewart M, Lasker J, *et al*. Three-dimensional optical tomographic brain imaging in small animals, part 1: hypercapnia. *J Biomed Optics* 9(5) (2004), 1046–1062.

18. Kobashi S, Tsuda Y, Yanagida T and Hata Y. Hemodynamic response latency analysis using wavelet transform in event-related functional MRI. *International Journal of Intelligent Computing in Medical Sciences and Image Processing* 2 (2008), 197–208.

19. Zhao Y, Shan T, Chi Z and Jiang H. Thermoacoustic tomography of germinal matrix hemorrhage in neonatal mouse cerebrum. *Journal of X-ray Science and Technology* 28(1) (2020), 83–93.

20. Carmi L, Tendler A, Bystritsky A, *et al*. Efficacy and safety of deep transcranial magnetic stimulation for obsessive- compulsive disorder: A prospective multicenter randomized double-blind placebo-controlled trial. *American Journal of Psychiatry* 176(11), (2019), 931–938.

21. Lusicic A, Schruers K.R, Pallanti S and Castle D.J. Transcranial magnetic stimulation in the treatment of obsessive-compulsive disorder: current perspectives. *Neuropsychiatric Disease and Treatment* 14 (2018), 1721–1736.

22. Kessler RC, Bromet EJ. The epidemiology of depression across cultures. *Annu Rev Public Health*. 2013; 34:119-38.

23. Patel V, Chisholm D, Parikh R, Charlson FJ, Degenhardt L, Dua T, Ferrari AJ, Hyman S, Laxminarayan R, Levin C, Lund C, Medina Mora ME, Petersen I, Scott J, Shidhaye R, Vijayakumar L, Thornicroft G, Whiteford H. Addressing the burden of mental, neurological, and substance use disorders: key messages from Disease Control Priorities, 3rd edition. *Lancet*. 2016 Apr 16;387(10028):1672-8.

24. Wagner G, Matyas N, Titscher V, Greimel J, Lux L, Gaynes BN, Viswanathan M, Patel S, Lohr KN. Pharmacological and non-pharmacological treatments for major depressive disorder: review of systematic reviews. *BMJ Open*. 2017 Jun 14;7(6): e014912.

25. Sinyor M, Schaffer A, Levitt A. The sequenced treatment alternatives to relieve depression (STAR*D) trial: a review. *Can J Psychiatry*. 2010 Mar;55(3):126-35.

26. George MS, Grammer G, Janicak PG, Pascual-Leone A, Wirecki TS. The Clinical TMS Society Consensus Review and Treatment Recommendations for TMS Therapy for Major Depressive Disorder. *Brain Stimul.* 2016 May-Jun;9(3):336-346.

27. George MS, Lisanby SH, Avery D, McDonald WM, Durkalski V, Pavlicova M, Anderson B, Nahas Z, Bulow P, Zarkowski P, Holtzheimer PE 3rd, Schwartz T, Sackeim HA. Daily left prefrontal transcranial magnetic stimulation therapy for major depressive disorder: a sham-controlled randomized trial. *Arch Gen Psychiatry*. 2010 May;67(5):507-16.

28. Higgins ES, George MS: Brain Stimulation Therapies for Clinicians, 2nd ed. Washington, DC, American Psychiatric Association Publishing, 2020.

29. George MS, Wassermann EM, Williams WA, Callahan A, Ketter TA, Basser P, Hallett M, Post RM. Daily repetitive transcranial magnetic stimulation (rTMS) improves mood in depression. *Neuroreport*. 1995 Oct 2;6(14):1853-6.

30. George MS, Wassermann EM, Williams WA, Steppel J, Pascual-Leone A, Basser P, Hallett M, Post RM. Changes in mood and hormone levels after rapid-rate transcranial magnetic stimulation (rTMS) of the prefrontal cortex. *J Neuropsychiatry Clin Neurosci*. 1996 Spring;8(2):172-80.

31. George MS, Wassermann EM, Kimbrell TA, Little JT, Williams WE, Danielson AL, Greenberg BD, Hallett M, Post RM. Mood improvement following daily left prefrontal repetitive transcranial magnetic stimulation in patients with depression: a placebo-controlled crossover trial. *Am J Psychiatry*. 1997 Dec;154(12):1752-6.

32. O'Reardon JP, Solvason HB, Janicak PG, Sampson S, Isenberg KE, Nahas Z, McDonald WM, Avery D, Fitzgerald PB, Loo C, Demitrack MA, George MS, Sackeim HA. Efficacy and safety of transcranial magnetic stimulation in the acute treatment of major depression: a multisite randomized controlled trial. *Biol Psychiatry*. 2007 Dec 1;62(11):1208-16.

33. Berlim MT, van den Eynde F, Tovar-Perdomo S, Daskalakis ZJ. Response, remission and drop-out rates following high-frequency repetitive transcranial magnetic stimulation (rTMS) for treating major depression: a systematic review and meta-analysis of randomized, double-blind and sham-controlled trials. *Psychol Med*. 2014 Jan;44(2):225-39.

34. George MS. Whither TMS: A One-Trick Pony or the Beginning of a Neuroscientific Revolution. *Am J Psychiatry*. 2019 Nov 1;176(11):904-910.

35. Bestmann S, Baudewig J, Siebner HR, Rothwell JC, Frahm J. BOLD MRI responses to repetitive TMS over human dorsal premotor cortex. *Neuroimage*. 2005 Oct 15;28(1):22-9.

36. Shibasaki H. Human brain mapping: hemodynamic response and electrophysiology. *Clin Neurophysiol*. 2008 Apr;119(4):731-43.

37. Farzan F, Barr MS, Wong W, Chen R, Fitzgerald PB, Daskalakis ZJ. Suppression of gamma-oscillations in the dorsolateral prefrontal cortex following long interval cortical inhibition: a TMS-EEG study. *Neuropsychopharmacology*. 2009 May;34(6):1543-51.

38. Kozel FA, Tian F, Dhamne S, Croarkin PE, McClintock SM, Elliott A, Mapes KS, Husain MM, Liu H. Using simultaneous repetitive Transcranial Magnetic Stimulation/functional Near Infrared Spectroscopy (rTMS/fNIRS) to measure brain activation and connectivity. *Neuroimage*. 2009 Oct 1;47(4):1177-84.

39. Curtin A, Tong S, Sun J, Wang J, Onaral B, Ayaz H. A Systematic Review of Integrated Functional Near-Infrared Spectroscopy (fNIRS) and Transcranial Magnetic Stimulation (TMS) Studies. *Front Neurosci*. 2019;13-84.

40. Hoshi Y, Yamada Y. Overview of diffuse optical tomography and its clinical applications. *J Biomed Opt.* 2016 Sep;21(9):091312.

41. Lee CW, Cooper RJ, Austin T. Diffuse optical tomography to investigate the newborn brain. *Pediatr Res*. 2017 Sep;82(3):376-386.

42. Dai X, Zhang T, Yang H, Tang J, Carney PR, Jiang H. Fast noninvasive functional diffuse optical tomography for brain imaging. *J Biophotonics*. 2018 Mar;11(3).

43. Jiang H, Iftimia NV, Xu Y, Eggert JA, Fajardo LL, Klove KL. Near-infrared optical imaging of the breast with model-based reconstruction. *Acad Radiol*. 2002 Feb;9(2):186-94.

44. Yuan Z, Zhang Q, Sobel ES, Jiang H. Tomographic x-ray-guided three-dimensional diffuse optical tomography of osteoarthritis in the finger joints. *J Biomed Opt*. 2008 Jul-Aug;13(4):044006.

45. Zeff BW, White BR, Dehghani H, Schlaggar BL, Culver JP. Retinotopic mapping of adult human visual cortex with high-density diffuse optical tomography. *Proc Natl Acad Sci U S A*. 2007 Jul 17;104(29):12169-74.

46. Habermehl C, Holtze S, Steinbrink J, et al. Somatosensory activation of two fingers can be discriminated with ultra-high density diffuse optical tomography. *Neuroimage*. 2012;59(4):3201-3211.

47. First M, Williams JBW, Karg R, Spitzer RL. Structured clinical interview for DSM-5 (SCID). *American Psychiatric Press*. 2015.

48. Keel JC, Smith MJ, Wassermann EM. A safety screening questionnaire for transcranial magnetic stimulation. *Clin Neurophysiol*. 2001 Apr;112(4):720.

49. Pridmore S, Fernandes Filho JA, Nahas Z, Liberatos C, George MS. Motor threshold in transcranial magnetic stimulation: a comparison of a neurophysiological method and a visualization of movement method. *J ECT*. 1998 Mar;14(1):25-7.

50. Borckardt JJ, Nahas Z, Koola J, George MS. Estimating resting motor thresholds in transcranial magnetic stimulation research and practice: a computer simulation evaluation of best methods. *J ECT*. 2006 Sep;22(3):169-75.

51. Yang J, Zhang T, Yang H, Jiang H. Fast multispectral diffuse optical tomography system for in vivo three-dimensional imaging of seizure dynamics. *Appl Opt*. 2012 Jun 1;51(16):3461-9.

52. Jiang, H. Diffuse Optical Tomography: Principles and Applications. CRC Press, 2010.

53. Delpy DT, Cope M, van der Zee P, Arridge S, Wray S, Wyatt J. Estimation of optical pathlength through tissue from direct time of flight measurement. *Phys Med Biol*. 1988 Dec;33(12):1433-42.

54. Oldfield RC. The assessment and analysis of handedness: the Edinburgh inventory. *Neuropsychologia*. 1971 Mar;9(1):97-113.

55. Hada Y, Abo M, Kaminaga T, Mikami M. Detection of cerebral blood flow changes during repetitive transcranial magnetic stimulation by recording hemoglobin in the brain cortex, just beneath the stimulation coil, with near-infrared spectroscopy. *Neuroimage*. 2006 Sep;32(3):1226-30.

56. Cao TT, Thomson RH, Bailey NW, Rogasch NC, Segrave RA, Maller JJ, Daskalakis ZJ, Fitzgerald PB. A near infra-red study of blood oxygenation changes resulting from high and low frequency repetitive transcranial magnetic stimulation. *Brain Stimul.* 2013 Nov;6(6):922-4.

57. Shinba T, Kariya N, Matsuda S, Matsuda H, Obara Y. Increase of frontal cerebral blood volume during transcranial magnetic stimulation in depression is related to treatment effectiveness: A pilot study with near-infrared spectroscopy. *Psychiatry Clin Neurosci*. 2018 Aug;72(8):602-610.

58. Dean J, Keshavan M. The neurobiology of depression: An integrated view. *Asian J Psychiatr*. 2017 Jun;27:101-111.

59. Helm K, Viol K, Weiger TM, Tass PA, Grefkes C, Del Monte D, Schiepek G. Neuronal connectivity in major depressive disorder: a systematic review. *Neuropsychiatr Dis Treat*. 2018;14,2715-2737.

60. Chaudhury D, Liu H, Han MH. Neuronal correlates of depression. *Cell Mol Life Sci*. 2015 Dec;72(24):4825-48.

61. Barrett J, Della-Maggiore V, Chouinard PA, Paus T. Mechanisms of action underlying the effect of repetitive transcranial magnetic stimulation on mood: behavioral and brain imaging studies. *Neuropsychopharmacology*. 2004 Jun;29(6):1172-89.

62. Paus T, Barrett J. Transcranial magnetic stimulation (TMS) of the human frontal cortex: implications for repetitive TMS treatment of depression. *J Psychiatry Neurosci*. 2004 Jul;29(4):268-79.

63. Cole EJ, Stimpson KH, Bentzley BS, et al. Stanford Accelerated Intelligent Neuromodulation Therapy for Treatment-Resistant Depression. *Am J Psychiatry*. 2020;177(8):716-726.

64. Johnson KA, Baig M, Ramsey D, Lisanby SH, Avery D, McDonald WM, Li X, Bernhardt ER, Haynor DR, Holtzheimer PE 3rd, Sackeim HA, George MS, Nahas Z. Prefrontal rTMS for treating depression: location and intensity results from the OPT-TMS multi-site clinical trial. *Brain Stimul.* 2013 Mar;6(2):108-17.

65. McClintock SM, Reti IM, Carpenter LL, McDonald WM, Dubin M, Taylor SF, Cook IA, O'Reardon J, Husain MM, Wall C, Krystal AD, Sampson SM, Morales O, Nelson BG, Latoussakis V, George MS, Lisanby SH. Consensus Recommendations for the Clinical Application of Repetitive Transcranial Magnetic Stimulation (rTMS) in the Treatment of Depression. *J Clin Psychiatry*. 2018 Jan/Feb;79(1).

66. Herwig U, Padberg F, Unger J, Spitzer M, Schönfeldt-Lecuona C. Transcranial magnetic stimulation in therapy studies: examination of the reliability of "standard" coil positioning by neuronavigation. *Biol Psychiatry*. 2001 Jul 1;50(1):58-61.

67. Li CT, Cheng CM, Chen MH, Juan CH, Tu PC, Bai YM, Jeng JS, Lin WC, Tsai SJ, Su TP. Antidepressant Efficacy of Prolonged Intermittent Theta Burst Stimulation Monotherapy for Recurrent Depression and Comparison of Methods for Coil Positioning: A Randomized, Double-Blind, Sham-Controlled Study. *Biol Psychiatry*. 2020 Mar 1;87(5):443-450.

68. Herbsman T, Avery D, Ramsey D, Holtzheimer P, Wadjik C, Hardaway F, Haynor D, George MS, Nahas Z. More lateral and anterior prefrontal coil location is associated with better repetitive transcranial magnetic stimulation antidepressant response. *Biol Psychiatry*. 2009 Sep 1;66(5):509-15.

69. Weigand A, Horn A, Caballero R, Cooke D, Stern AP, Taylor SF, Press D, Pascual-Leone A, Fox MD. Prospective Validation That Subgenual Connectivity Predicts Antidepressant Efficacy of Transcranial Magnetic Stimulation Sites. *Biol Psychiatry*. 2018 Jul 1;84(1):28-37.

70. Jiang, S., Huang, J., Yang, H. *et al.* Neuroimaging of depression with diffuse optical tomography during repetitive transcranial magnetic stimulation. *Sci Rep* 11, 7328 (2021).

71. Https://www.nature.com/articles/s41598-021-86751-9.

Chapter 6: Conclusion

In this dissertation, we have demonstrated the structural and functional imaging capabilities of diffuse optical tomography imaging and the possibility of using it for guided imaging in healthy subjects and patients. Due to the thickness of the human skull, the effective depth for the human brain detection goes around 4 cm. In the first generation of diffuse optical tomography imaging system, it is only utilized in the clinical research environmental. That means the machine needs to be adapted by human. In the hospital experiment, the requirement should let the machine adapt to the patient.

In summary, for the TMS &DOT and delirium human study, we demonstrate the ability of a novel DOT system to capture cerebral hemodynamic activity in delirious and healthy individuals. As our study continues, we plan to further enroll subjects to increase our sample sizes, conduct a functional connectivity analysis to study any dysregulation that may occur within the prefrontal cortex or other regions of the brain, and conduct formal statistical analyses.

Appendix A: Copyright Permissions

The permission below is for the use of materials in Chapter 1 through Chapter 5. Some of the drawings were done in Biorender, with an academic subscription, which comes with publishing rights. Biorender is appropriately cites in these figures (Created with BioRender.com). The second permission is to reproduce materials published in Scientific Report and Journal of X-Ray Science and Technology. The email approvals and the statement of the Creative Commons license for the IOS Press have presented in this section.

bio RENDER

Licensing and Usage

	Basic (Free) Account*	Academic Subscription	Industry Subscription
Educational Uses:			
Academic poster	✓	✓	✓
Thesis/dissertation (unpublished)	✓	✓	✓
Internal meetings (lab or team)	✓	✓	✓
Conference presentation	✓	✓	✓
Assignment/exam	✓	✓	✓
Teaching slides	✓	✓	✓
Personal blog/website posts	✓	✓	✓
Personal social media posts	✓	✓	✓
Publishing Uses:			
Journal publication		✓	✓
Textbook publication (< 5 figures)		✓	✓
Published thesis		✓	✓
Commercial Uses:			
Any uses that generate profit			✓
Textbook publication (5+ figures)			✓
Trade show materials (e.g. brochures)			✓
Information packages/user guides			✓

*Watermark must be included in exported figure
*Free trial on a premium plan recommended for print uses
For use cases not listed here, please go to **biorender.com/contact**

Conditions for Publication rights:

1. The figure was exported under a **paid subscription.**
2. Citation of "**Created with BioRender.com**" appears somewhere in the publication.

› Sci Rep. 2021 Apr 1;11(1):7328. doi: 10.1038/s41598-021-86751-9.

Neuroimaging of depression with diffuse optical tomography during repetitive transcranial magnetic stimulation

Shixie Jiang [# 1], Jingyu Huang [# 2], Hao Yang [2], Ryan Wagoner [1], F Andrew Kozel [1 3], Glenn Currier [1], Huabei Jiang [4]

Affiliations – collapse

Affiliations

1 Department of Psychiatry and Behavioral Neurosciences, University of South Florida, Tampa, FL, USA.
2 Department of Medical Engineering, University of South Florida, 4202 E. Fowler Avenue, ENG 030, Tampa, FL, USA.
3 Department of Behavioral Sciences and Social Medicine, Florida State University, Tallahassee, FL, USA.
4 Department of Medical Engineering, University of South Florida, 4202 E. Fowler Avenue, ENG 030, Tampa, FL, USA. hjiang1@usf.edu.
# Contributed equally.

PMID: 33795763 PMCID: PMC8016845 DOI: 10.1038/s41598-021-86751-9

Free PMC article

permission or licencse

Journalpermissions <journalpermissions@springernature.com>
收件人: Jingyu Huang
周二 2022/11/22 11:54

Dear Jingyu,

Thank you for your recent email. Springer Nature journal authors may reuse their article's Version of Record, in whole or in part, in their own thesis without any additional permission required, provided the original publication is properly cited and includes the following acknowledgement '"Reproduced with permission from Springer Nature". This includes the right to make a copy of your thesis available in your academic institution's repository, or other repository required by your awarding institution. For more information please visit see our FAQs here.

If your awarding institution requires formal permission, please locate your article on either nature.com or link.springer.com. At the end of the article page you will find the 'Reprints and Permissions' link; clicking on this will redirect you to our CCC RightsLink service where you may input the details of your request. Please ensure you select "reuse in a thesis/dissertation' as your type of use, and to tick the box that asks whether you are the author.

During the process, you will need to set up an account with RightsLink. You will be able to use your RightsLink account in the future to request permissions from Springer Nature and from other participating publishers. RightsLink will also email you confirmation of your request with a link to your printable licence.

If you have any further questions, please do not hesitate to get in touch.
Kind Regards,

Elise

Elise Lagden
Permissions Assistant
SpringerNature
The Campus, 4 Crinan Street, London N1 9XW, United Kingdom
E elise.lagden@springernature.com
http://www.nature.com
http://www.springernature.com

J Xray Sci Technol. 2021;29(5):891-902. doi: 10.3233/XST-210900.

Three-dimensional optical imaging of brain activation during transcranial magnetic stimulation

Jingyu Huang [1], Shixie Jiang [2], Ryan Wagoner [2], Hao Yang [1], Glenn Currier [2], Huabei Jiang [1]

Affiliations + expand

PMID: 34397443 DOI: 10.3233/XST-210900

Case #01748702 - Open Access article permissions

1

Dear J Huang,

Thank you for contacting CCC earlier, it was a pleasure speaking to you. As promised, I am reaching back out to provide you the caption of the page where the rightsholder indicates that permission is not required because the work is Open Access under a CC BY license. Please find it attached.

The following messaging is also provided by the publisher, directly on the page where the article in question is published: "*This article is licensed under a Creative Commons Attribution 4.0 International License, which permits use, sharing, adaptation, distribution and reproduction in any medium or format, as long as you give appropriate credit to the original author(s) and the source, provide a link to the Creative Commons licence, and indicate if changes were made. The images or other third party material in this article are included in the article's Creative Commons licence, unless indicated otherwise in a credit line to the material. If material is not included in the article's Creative Commons licence and your intended use is not permitted by statutory regulation or exceeds the permitted use, you will need to obtain permission directly from the copyright holder. To view a copy of this licence, visit http://creativecommons.org/licenses/by/4.0/.*"

I hope this information helps and let me know if you need additional assistance with anything related to our services.

Best regards,
Daniel

Daniel Ilies
Customer Account Specialist
Copyright Clearance Center
222 Rosewood Drive
Danvers, MA 01923
www.copyright.com
Toll Free US +1.855.239.3415

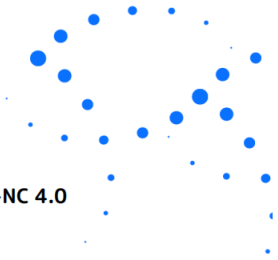

IOS Press

License to publish under Creative Commons CC BY-NC 4.0

Publisher/Licensee IOS Press B.V., Nieuwe Hemweg 6 B, 1013 BG Amsterdam, The Netherlands

Definitions :

• Published version of the article = peer reviewed and typeset article in the publisher's format

• Author's Original paper / Article = submitted version of the manuscript prior to peer-review

1. Grant of Rights

By accepting this License to Publish, you hereby grant the Publisher the exclusive right, unlimited in time and territory, to any commercial use: to publish, republish, transmit, sell, distribute, store and otherwise use the Article in whole or in part, including abstracts thereof, in all languages and in all media of expression now known or later developed, and to license or permit others (including but not limited to Reproduction Rights Organisations such as the Copyright Clearance Centre) to do so. Furthermore, you grant the Publisher the right to use the Article in whole or in part, within the Journal, as stand-alone and/or with other related material in databases, data networks and for multimedia purposes including the right to alter the Article if necessary for these purposes.

2. Use of Article under CC BY-NC

2.1. You acknowledge and agree that the Article will be published by the Publisher in the Journal and made freely available to users under the terms of the Attribution Non Commercial 4.0 Creative Commons License (http://creativecommons.org/licenses/by-nc/4.0/legalcode) (the "CC BY-NC") which permits use, distribution and reproduction in any medium, provided that the Article is properly cited and is not used for commercial purposes.

2.2. The Publisher will clearly mark the Article being published under the CC BY-NC License in the Journal and link to the terms of the CC BY-NC. The Publisher will include a copyright notice of the copyright holder to the Article.

3. Rights Retained and Self-Archiving

3.1. You retain all copyright in the Article.

3.2. Your final published version of the Article (Published Article) will be made available on the Journal's website immediately upon publication against payment of the respective Open Access Fee. The exchange of the published version by digital file-sharing or similar means is Non-Commercial provided there is no payment of monetary compensation in connection with the exchange.

3.3. You retain the right to post a copy of the originally submitted version of your article ('Author's Original'), the accepted version of your article and / or the final published version of the Article (Published Article) to your personal, your institute's, company's or funding agency's website and/or in an online repository (such as arXiv, BioRxiv or

Latest version: November 22, 2022

Appendix B: IRB Approvals

This appendix contains the Institutional Review Boards (IRBs) of USF and Tampa General Hospital. Protocols followed the protection of human subject in clinical trial. The various approval certificates and procedural changes are shown.

USF
UNIVERSITY OF SOUTH FLORIDA

RESEARCH INTEGRITY AND COMPLIANCE
Institutional Review Boards, FWA No. 00001669
12901 Bruce B. Downs Blvd., MDC035 • Tampa, FL 33612-4799
(813) 974-5638 • FAX (813) 974-7091

1/29/2018

Glenn Currier, M.D., M.P.H
Psychiatry and Behavioral Neurosciences
USF Department of Psychiatry
3515 E Fletcher Ave
Tampa, FL 33613

RE: **Expedited Approval for Initial Review**
IRB#: Pro00032521
Title: Optical imaging during transcranial magnetic stimulation for treatment of depression

Study Approval Period: 1/27/2018 to 1/27/2019

Dear Dr. Currier:

On 1/27/2018, the Institutional Review Board (IRB) reviewed and **APPROVED** the above application and all documents contained within, including those outlined below.

Approved Item(s):
Protocol Document(s):
Protocol - IRB_DOT_TMS_Depression (1 23 2018).doc

Consent/Assent Document(s)*:
Consent - IRB_DOT_TMS_Depression (1 23 2018).docx.pdf

*Please use only the official IRB stamped informed consent/assent document(s) found under the "Attachments" tab. Please note, these consent/assent documents are valid until the consent document is amended and approved.

It was the determination of the IRB that your study qualified for expedited review which includes activities that (1) present no more than minimal risk to human subjects, and (2) involve only procedures listed in one or more of the categories outlined below. The IRB may review research through the expedited review procedure authorized by 45CFR46.110 and 21 CFR 56.110. The research proposed in this study is categorized under the following expedited review category:

(4) Collection of data through noninvasive procedures (not involving general anesthesia or sedation) routinely employed in clinical practice, excluding procedures involving x-rays or microwaves. Where medical devices are employed, they must be cleared/approved for marketing.

(5) Research involving materials (data, documents, records, or specimens) that have been collected, or will be collected solely for non-research purposes (such as medical treatment or diagnosis).

(6) Collection of data from voice, video, digital, or image recordings made for research purposes.

Your study qualifies for a waiver of the requirements for the informed consent process as outlined in the federal regulations at 45CFR46.116 (d) which states that an IRB may approve a consent procedure which does not include, or which alters, some or all of the elements of informed consent, or waive the requirements to obtain informed consent provided the IRB finds and documents that (1) the research involves no more than minimal risk to the subjects; (2) the waiver or alteration will not adversely affect the rights and welfare of the subjects; (3) the research could not practicably be carried out without the waiver or alteration; and (4) whenever appropriate, the subjects will be provided with additional pertinent information after participation.

As the principal investigator of this study, it is your responsibility to conduct this study in accordance with IRB policies and procedures and as approved by the IRB. Any changes to the approved research must be submitted to the IRB for review and approval via an amendment. Additionally, all unanticipated problems must be reported to the USF IRB within five (5) calendar days.

We appreciate your dedication to the ethical conduct of human subject research at the University of South Florida and your continued commitment to human research protections. If you have any questions regarding this matter, please call 813-974-5638.

Sincerely,

E. Verena Jorgensen, M.D., Chairperson
USF Institutional Review Board

Investigator:	Shixie Jiang, MD
Study Title:	Neuroimaging of delirium with diffuse optical tomography
IRB #:	STUDY000832
Research Office #:	20-0259

The above referenced study has been reviewed and approved by the Tampa General Hospital (TGH) Office of Clinical Research (OCR). Further, TGH OCR has determined the protected health information requested from TGH for the above referenced study is reasonably necessary for Research, as defined in 45 CFR § 164.501. The information below is a set of expectations set forth for the Investigator and study staff. Any deviation from these expectations may result in the withdrawal of study approval at TGH.

- Study activity may commence. **Please note that Jingyu Huang, Hao Yang, and Huabei Jiang are not permitted to view identifiable patient data until they have finished the credentialing process.**

- Subsequent approval and study continuation are conditioned on timely receipt of approved continuing review documents from the IRB of record.

- Notify TGH Research at researchregulatory@tgh.org for the following:
  - Any changes to the protocol or informed consent prior to IRB submission .
  - All other documents submitted for IRB review must be submitted to TGH within three (3) business days.
  - Serious adverse events (SAE) and unanticipated problems (UAP) must be reported within 24 hours upon notification of event.
  - Any changes to study status (e.g. enrollment closure, pending study closure or study closed) must be submitted within 24 hours of the notification.
  - Any changes to study personnel (addition or removal)
    - Study personnel added after initial IRB approval must be credentialed by TGH OCR prior to completing any study-related activities.

- Patient activity must be captured in TGH's Clinical Trial Management System (CTMS) and Epic for all protocol related activity at TGH. It is the Investigator's responsibility to ensure current study activity is captured in CTMS and Epic within 24 hours of activity.

- In conducting this protocol at TGH you are required to follow the requirements listed in the Investigator Manual TGH OCR-103 policy.

- **For CORE Studies only:** Please await instructions from CORE Leadership on when accrual can commence.

Sincerely,

[redacted]

Tracy Popp, MBA, CHRC, CCRP, CRCP
Sr. Director, Clinical Research
Tampa General Hospital
cc: TGH File